Detailed maps of tropical forest types are within reach: Forest tree communities for Trinidad and Tobago mapped with multiseason Landsat and multiseason fine-resolution imagery

E.H. Helmer [a,*], Thomas S. Ruzycki [b], Jay Benner [b], Shannon M. Voggesser [b], Barbara P. Scobie [c], Courtenay Park [c,1], David W. Fanning [d], Seepersad Ramnarine [c]

[a] International Institute of Tropical Forestry, USDA Forest Service, Río Piedras, PR 00926, United States
[b] Center for Environmental Management of Military Lands, Colorado State University, Fort Collins, CO 80523, United States
[c] Trinidad and Tobago Forestry Division, Long Circular Road, St. Joseph, Trinidad and Tobago
[d] Fanning Software Consulting, 1645 Sheely Drive, Fort Collins, CO 80526, United States

ARTICLE INFO

ABSTRACT

Tropical forest managers need detailed maps of forest types for REDD+, but spectral similarity among forest types; cloud and scan-line gaps; and scarce vegetation ground plots make producing such maps with satellite imagery difficult. How can managers map tropical forest tree communities with satellite imagery given these challenges? Here we describe a case study of mapping tropical forests to floristic classes with gap-filled Landsat imagery by judicious combination of field and remote sensing work. For managers, we include background on current and forthcoming solutions to the problems of mapping detailed tropical forest types with Landsat imagery. In the study area, Trinidad and Tobago, class characteristics like deciduousness allowed discrimination of floristic classes. We also discovered that we could identify most of the tree communities in (1) imagery with fine spatial resolution of ⩽1 m; (2) multiseason fine resolution imagery (viewable with Google Earth); or (3) Landsat imagery from different dates, particularly imagery from drought years, even if decades old, allowing us to collect the extensive training data needed for mapping tropical forest types with "noisy" gap-filled imagery. Further, we show that gap-filled, synthetic multiseason Landsat imagery significantly improves class-specific accuracy for several seasonal forest associations. The class-specific improvements were better for comparing classification results; for in some cases increases in overall accuracy were small. These detailed mapping efforts can lead to new views of tropical forest landscapes. Here we learned that the xerophytic rain forest of Tobago is closely associated with ultramafic geology, helping to explain its unique physiognomy.

Published by Elsevier B.V.

1. Introduction

Tropical forest managers need to produce detailed forest maps for REDD+, which is a mechanism that gives countries financial incentives for Reducing Emissions from Deforestation and Degradation and managing forests to sustain biodiversity and enhance carbon stocks (REDD+) (Wertz-Kanounnikoff and Kongphan-apirak, 2009; Phelps et al., 2010). Maps of forest types, including tree community distributions, are essential for many related management questions. Vegetation mapping is often a first step in regional planning for biodiversity conservation (Scott et al., 1993). In addition, as the carbon storage of forests becomes more variable across a landscape, estimates of carbon storage that are based on forest inventory plots become less precise and accurate. Estimates are improved, and the number of forest plots can be reduced, when forests are stratified into more homogenous units, such as by forest type (Estrada, 2011).

No example exists of a country-wide map of tropical forest tree communities at Landsat scale. At the floristic level prior Landsat-based maps do not consider clouds and use only one season of imagery (Chust et al., 2006; Sesnie et al., 2008). Mapping for REDD+ and other management, however, requires that gaps from clouds in remotely sensed imagery be filled. *Gap-filled* imagery is mosaicked or composited from many scene dates to fill image gaps that stem from failure of the scan-line corrector on the Landsat 7 Enhanced Thematic Mapper (ETM+) (Wulder et al., 2008). We also use the term to include filling gaps from clouds as in Helmer and Ruefenacht (2005). Tropical forest mapping with gap-filled Landsat imagery has been limited to mapping forest physiognomic types

(Kennaway and Helmer, 2007; Helmer et al., 2008; Kennaway et al., 2008), forest cover or change (Hansen et al., 2008; Lindquist et al., 2008), or forest vertical structure, disturbance type and wetland type (Helmer et al., 2010).

By tree communities we mean forest *associations* (*sensu* Jennings et al., 2009), which are species-specific assemblages. They are distinct from more general and easily mapped physiognomic classes (*i.e. formations*, where forests are classified with modifiers like deciduous, semi-evergreen, evergreen or montane; closed or open; broad-leaved or needle-leaved, etc.). Associations are also more detailed than life zones (*sensu* Holdridge, 1967). Life zones are climatic classes; they only generally relate to species composition (Pyke et al., 2001). Trinidad has four life zones (nine including transitional zones) (Nelson, 2004), compared with seven forest formations or about 26 forest associations (counting mature native forests, plantations and bamboo) (Beard, 1946a).

Major challenges when mapping forest associations are that (1) most Landsat imagery over tropical forests has clouds or other data gaps; (2) at first glance different tree communities look the same in air photos or have similar signatures in multispectral satellite imagery; (3) residual errors from gap-filling make the spectral signatures of classes more variable, increasing spectral overlap among different forest types; and (4) ground-based reference data for training image classifications are sparse. Moreover, previous work mapping tropical forest types with Landsat imagery uses some noncommercial computer programs that few staff have experience with.

How can managers meet these challenges and produce detailed maps of tropical forest types for REDD+ with Landsat? Our goals are to help answer that question. Some unexpectedly promising findings suggest that simple steps can improve results. We present a case study from Trinidad and Tobago, and for managers we give some background on current and forthcoming solutions to the above challenges. We also specifically test the following (the first two questions have not been previously tested):

1. Whether tropical forest associations can be mapped with decision-tree classification of gap-filled Landsat imagery and reference data supplemented by fine resolution imagery like that viewable with Google Earth (Google, 2010) (Version 5.2) [Software], which is available from http://www.google.com/earth/index.html.
2. Whether three gap-filled Landsat images made from three 1980s scenes with different phenologies would be redundant with one another, or would incrementally improve classification models of tropical forest association, when each gap-filled image comes from using two of the three scenes to fill gaps in the third scene, yielding a form of synthetic multiseason imagery.
3. Whether gap-filled imagery of the thermal band improves mapping of low-density urban lands.

2. Background

2.1. Filling clouds and other data gaps in Landsat imagery

To fill clouds and other data gaps in Landsat imagery, image data from different dates are combined after applying atmospheric correction, or after normalization to a reference scene. The reason is that the images from different dates have different atmospheric conditions, sensor calibration, sun elevation, view angle and vegetation or soil phenology. Without normalizing the data, the spectral signatures of a given forest type will vary greatly among the pixels sourced from different image dates, increasing spectral confusion among types. To normalize these signatures, normalization models use: (1) nonlinear relationships between clear overlapping

pixels of fill scenes and reference scenes (Helmer and Ruefenacht, 2005); (2) linear relationships between clear overlapping pixels that are somehow localized, *e.g.* drawn from a small surrounding window (Howard and Lacasse, 2004; Chen et al., 2011) and thereby at the scene level are not linear; (3) localized linear relationships based on the relationships between overlapping pixels of two images with coarse spatial but fine temporal resolution that are dated closely to the base and fill Landsat scenes (Roy et al., 2008); or, potentially, (4) the phenological pattern of past imagery.

2.2. Defining the space in which forest types are separable

Different forest types may only display subtle spectral differences in multispectral imagery from the peak of a growing season or when forested wetlands are not inundated. To help distinguish spectrally similar forest types, image bands from different times or from ancillary environmental data can be added to improve the potential to discriminate types. For example, multiseason imagery reduced confusion among tropical forest formations in Landsat imagery (Bohlman et al., 1998; Tottrup, 2004), and monthly composites of imagery with coarse spatial resolution (250 m–1 km) supported large-area mapping of tropical forest formations (Gond et al., 2011).

Adding data bands of environmental variables is like adding image bands from other times. Topography, for example, helps distinguish spectrally similar forest types when they occur in different environments (Skidmore, 1989). Another mapped variable that helps predict tree species composition is substrate. Limestone and serpentine geological substrates, or acid soils, are classic examples (Beard, 1946a; Ewel and Whitmore, 1973; Pyke et al., 2001). Studies use geological substrate when mapping tropical forest type with satellite imagery (Helmer et al., 2002; Chust et al., 2006; Kennaway and Helmer, 2007). Geographic position also explains variation in the composition of tropical forest tree species (Chinea and Helmer, 2003; Chust et al., 2006) and is also used as a mapping predictor layer (Chust et al., 2006; Sesnie et al., 2008).

Like adding image bands from different seasons, adding image bands from other years or decades also helps distinguish tropical forest types by helping to distinguish successional stage (Kimes et al., 1999; Helmer et al., 2000), or disturbance type (Helmer et al., 2010). Disturbance type and land use affect the species composition of secondary tropical forests (Aide et al., 1996; Chinea, 2002; Chinea and Helmer, 2003). With long time series of gapfilled Landsat we can map classes of tropical forest disturbance type and age that relate to young forest species composition (Helmer et al., 2010; Larkin et al., 2012). Mapping old forest type and forest disturbance history from a long time series creates maps of "forest harvest legacies" *sensu* Sader and Legaard (2008). For REDD, estimates of forest biomass from lidar or plot data may then be averaged over patches of similar forest type or disturbance history (*e.g.* Helmer et al., 2009; Nelson et al., 2009) to estimate forest carbon storage over landscapes.

To effectively incorporate ancillary data that maps environmental variables into classifications, machine learning classification algorithms (and expert systems) are used. They outperform linear methods like maximum likelihood classification and do not assume that class spectral distributions are parametric. Commonly used algorithms are decision trees (Lees and Ritman, 1991; Hansen et al., 1996), neural networks (Chen et al., 1995; Foody et al., 1995), and support vector machines (Brown et al., 2000).

2.3. Augmenting sparse plot data with high-resolution imagery

Studies have mapped forest types by predicting their spatial distributions with ordination of plot data against mapped environmental gradients and satellite imagery (Ohmann and Gregory,

2002; Chust et al., 2006). Plot data from systematic inventories, however, are often not available. They often miss rare forest types, and they may not include enough plots to capture the spatial and spectral variability of forest associations. Complex climatic, edaphic, anthropogenic and dispersal factors all affect the spatial patterns of forest associations. Moreover, residual errors in the normalization models used to produce gap-filled imagery add noise (*i.e.* variability) to the spectral signature of each forest type, increasing spectral confusion among types. When classifying gap-filled Landsat imagery with decision trees and ancillary data, training data must represent the spatial and spectral range of each class, including observations from the different dates that compose a gap-filled image (Helmer and Ruefenacht, 2007). This statement implies the need for thousands of well-distributed classification training points, more points than are normally available from field plots. Sesnie et al. (2008), for example, had only 144 forest plots, but they collected thousands of training pixels for each lowland forest association from 1:60,000-scale black and white air photos.

3. Methods

3.1. Study area

The Republic of Trinidad and Tobago (10°41′N, 61°13′N) is a southeastern Caribbean country that includes two main islands, Trinidad and Tobago, and many small outer islands that together encompass 5133 km² (Fig. 1). Trinidad lies on the South American continental shelf and was once part of South America. Its vegetation is similar to that of northeastern South America. Tobago

formed by obduction at the edge of this shelf (Snoke et al., 2001a). Its flora has an Antillean influence but is more closely related to that of South America (Oatham and Boodram, 2006).

With a tropical climate, mean annual temperatures range from 21 to 27 °C in Trinidad and 23 to 27 °C in Tobago. Total precipitation ranges from about 1370–2900 mm year^{-1} on Trinidad and 1630–2530 mm year^{-1} on Tobago (Hijmans et al., 2005) and includes a dry season from January to April and a wet season from July to November; May to June and December are transitional months. Most forests are moist broadleaved seasonal evergreen, but forests also include hardleaved evergreen coastal, deciduous, semi-evergreen, montane evergreen, and wetland formations (Beard, 1944a, 1946a).

Elevations reach 940 m in the Northern Range of Trinidad (Farr et al., 2007), which has steep topography and free draining soils developed over metamorphic rock. Elevations reach 320 m in Trinidad's smaller Central Range (Farr et al., 2007), which is composed of marine sedimentary rocks. Some limestone outcrops and hills occur in the Northern and Central Ranges. Alluvial and terrace lowlands, with clay to sandy clay soils and restricted drainage, occur between the Northern and Central ranges and southeast of the Central Range. The Southern Range is a series of hills that rise to about 280 m. Soils of these hills and of the southern lowlands have formed mainly over sandstones and siltstones. Southwestern Trinidad is mainly marine sedimentary (Donovan, 1994; Day and Chenoweth, 2004).

On Tobago, elevations range from sea level to about 570 m on the Main Ridge. Surficial rocks in Tobago's northeastern third, including the Main Ridge, are metavolcanic schist. Meeting the
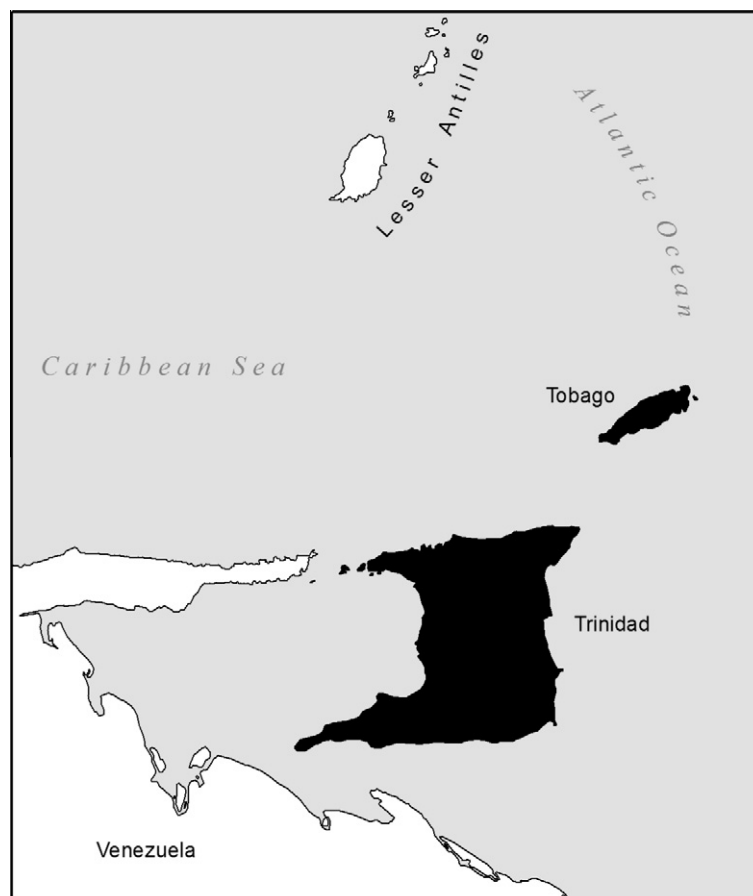

Fig. 1. The study covered the Republic of Trinidad and Tobago.
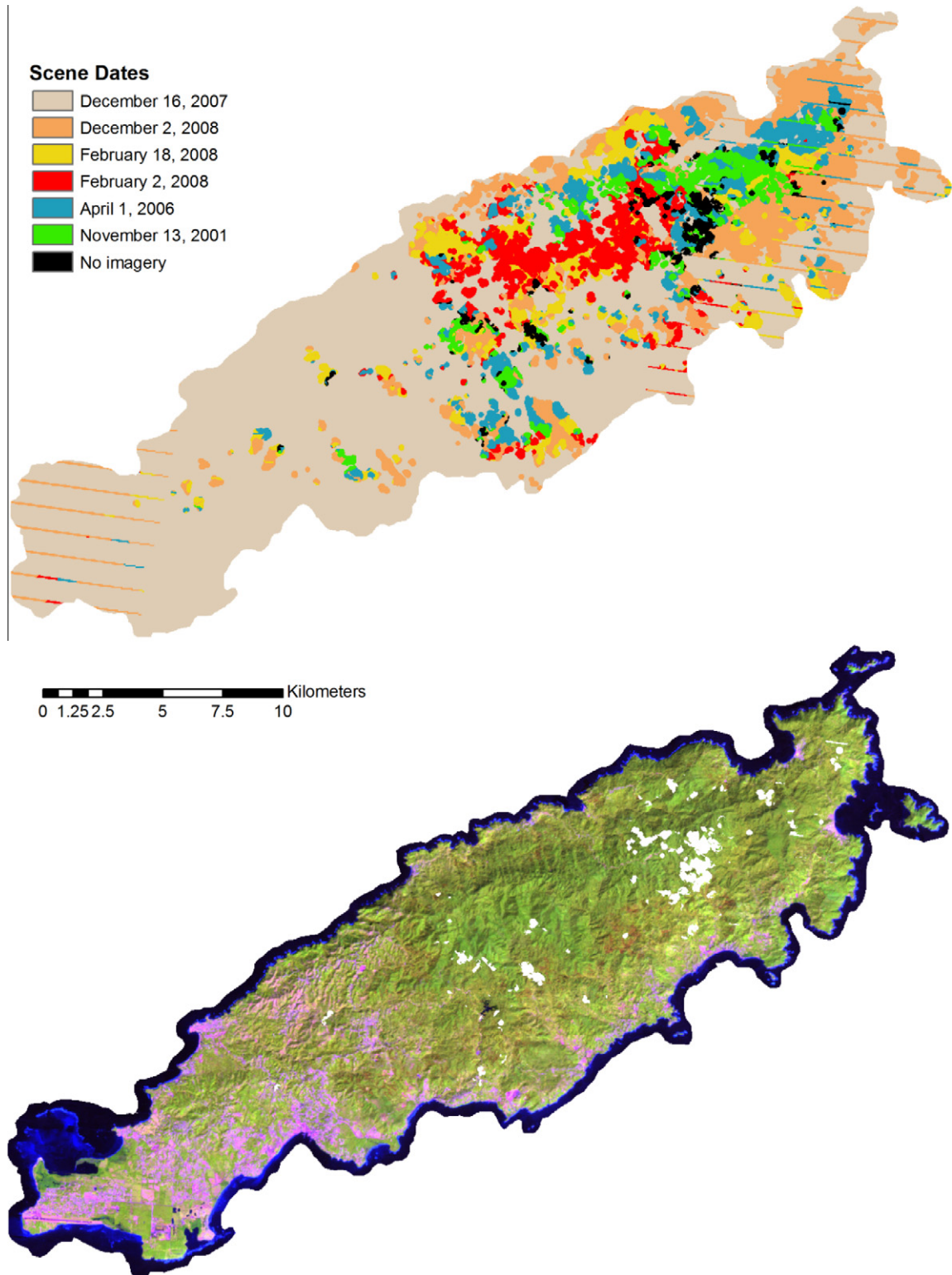
Fig. 2. Cloud and scan gaps in Landsat 7 ETM+ scenes were filled with images from other dates. The *fill* images first underwent regression tree normalization (Helmer and Ruefenacht, 2005) to the *base* scene. Shown here are: (a) the date band for Tobago; (b) the gap-filled image for Tobago; (c) the date band for Trinidad; and (d) the gap-filled image for Trinidad. Images display bands 5, 4 and 3 in RGB.

Main Ridge to the south are igneous rocks, including some serpentine substrates in ultramafic intrusives. The lowlands further southwest are sedimentary rocks; the southwest point is limestone (Maxwell, 1948; Jackson and Donovan, 1994; Snoke et al., 2001b).

3.2. Gap-filled multiseason, multidecade Landsat imagery

All Landsat imagery over Trinidad and Tobago has cloud or scan gaps. We made recent gap-filled ETM+ imagery for Trinidad and Tobago, filling gaps from clouds, scan lines and scene edges in

Scene Dates

- December 16, 2007
- March 5, 2002
- January 29, 2001
- April 17, 2006
- January 30, 2007
- March 21, 2008
- February 3, 2006
- February 11, 2003
- January 24, 2008
- October 25, 2000
- No imagery

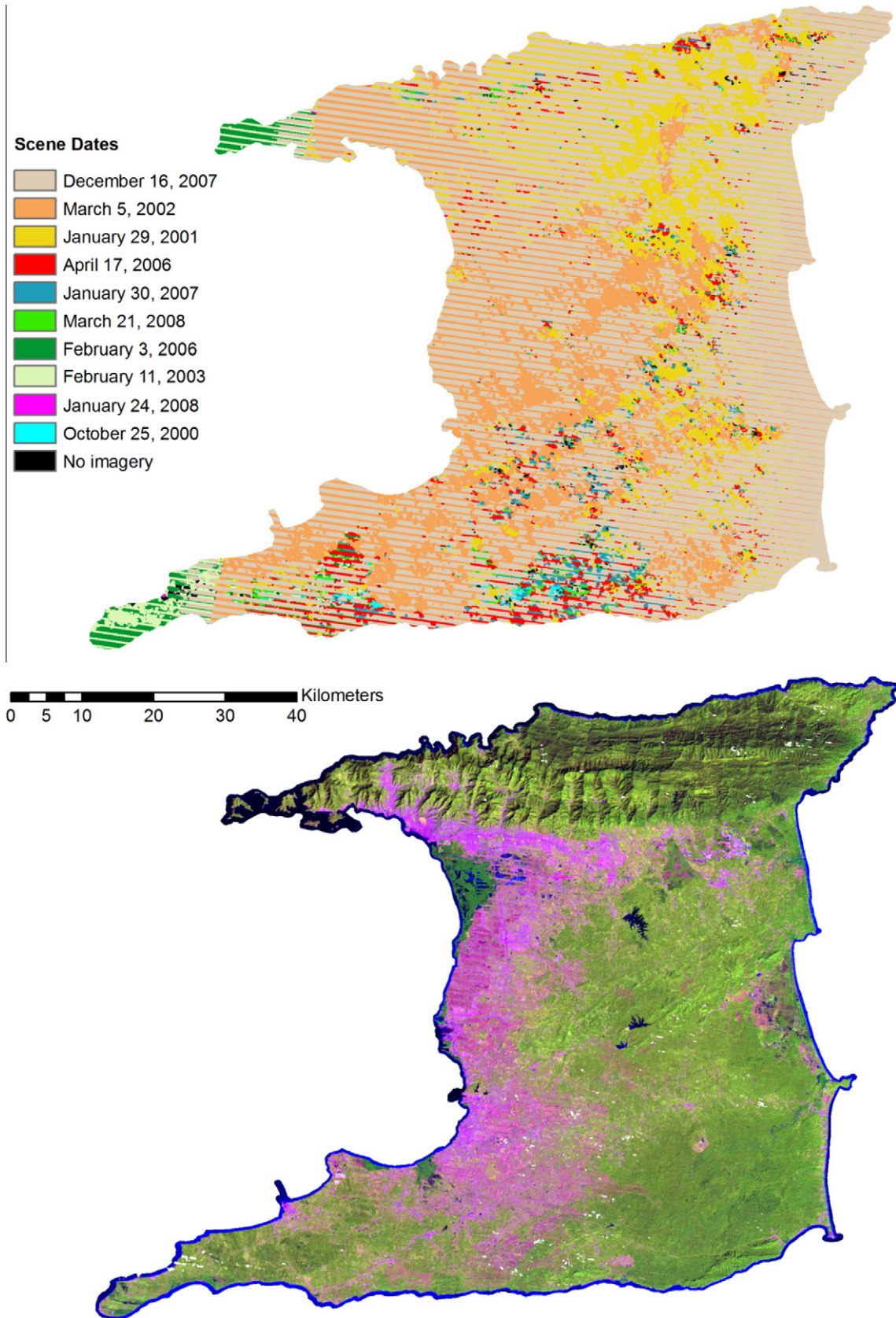**Fig. 2** (*continued*)

reference scenes from the early dry season of 2007 (December) with image data from *fill* scenes (Table 3 and Fig. 2). In our prior work mapping physiognomic forest types, image gaps came only from clouds, as we used imagery dated before late May of 2003. Here scan gaps added uncertainty to our ability to map forest associations. Each fill scene first underwent regression-tree

normalization to the 2007 data. This nonlinear normalization minimizes the atmospheric, phenological and sensor differences between the base and fill scenes and is described elsewhere (Helmer and Ruefenacht, 2005, 2007).

In Trinidad, we mapped land cover with the 2007 gap-filled imagery. We then mapped forest association with separate classification models that were applied only to forests. For these classification models of forest association, we added gap-filled imagery from the late dry season (see below). Tobago has far fewer mature forest associations than Trinidad; there we simultaneously mapped land cover and forest associations with the 2007 gap-filled imagery.

We used the early dry season imagery for land-cover mapping because forest is most distinct from nonforest then: deciduous forests are still leafed out, making them more spectrally distinct from nonforest. In contrast in the late dry season, leaf loss for deciduous tropical tree species peaks, causing confusion between deciduous forest and nonforest. In the wet season, flooding helps distinguish forested wetlands, but dense herbaceous cover is greened up and may be spectrally similar to young forest.

In the course of this work we observed that imagery from the late dry season (late March–early May) might be helpful for distinguishing among the many seasonal forest associations in Trinidad, most of which would simply be classified as moist forests in the life zone system. Consequently, for mapping forest type we made three gap-filled images from the mid- to late dry season for mapping forest type with three Landsat TM scenes from the years 1985–1987 (Table 3). Because each of these 1980s images displayed slightly different phenology, we sought gap-filled images that represented the unique phenology of each scene, and so each scene served as a base scene to which we then normalized the other two scenes. Whether this form of synthetic multiseason imagery would improve results had not been tested for mapping tropical forest associations.

Another reason for using imagery from the 1980s is that adding image bands from previous decades to the set of spectral bands being classified helps distinguish mature and old-growth tropical forest from secondary forest (Kimes et al., 1999; Helmer et al., 2000). Being ∼20 years old, the 1980s data might help distinguish forest younger than ∼15–20 years old in the 1980s (up to ∼35–40 years old in 2007) from older ("mature") forests (assuming that forest regrowth becomes indistinct from mature forest after about 15–20 years).

3.3. Cloud masking

In making the mosaics, we masked clouds and cloud shadows with: (1) an algorithm that identified clouds and potential cloud shadows with a series of models in ERDAS Imagine and a short routine in Interactive Data Language (IDL); (2) an IDL program that identified actual cloud shadow from clouds, potential cloud shadow and solar geometry which was partly based on Choi and Bindschadler (2004); and (3) manual refinement. The algorithm requires some clear area over land and water, and clouds must be no warmer than water. It ignores snow and ice.

The algorithm to identify clouds and potential cloud shadows uses *Histogram Fitting for Mapping* (HFM), which Helmer et al. (2009) describe for making a forest mask with image-specific thresholds found from image histograms. Water and land pixels are identified with the Shuttle Radar Topography Mission (SRTM) Water Body Dataset (SWBD) (NGA, 2003). Next, IDL fits a normal distribution to the histogram of the thermal infrared band (TIR$_{band6}$) for water pixels, and then for land pixels. Cool and warm clouds are found as pixels cooler than or as cool as most water pixels, respectively, or cooler than land if land is cooler than water. Clouds are preliminarily masked from the image, and the parame-

ters are again estimated for each band by fitting a normal distribution to the new histograms of water and land. Pixels are then masked from the identified clouds if they are darker than or as dark as most water in the second shortwave-infrared band (SWIR$_{band7}$), removing warm or shallow water. Cool land is then removed from the cloud mask by removing pixels that are as dark as most land in the blue band. Potential cloud shadow over land is mapped as areas that are darker in bands 4 and 5 than most land.

Next, each cloud patch is gradually shifted in the direction of the shadows. The distance of maximum overlap between pixels in the shifting cloud patch and pixels of potential cloud shadow is found as the peak of the distribution of overlapping pixels for different distances. The shifted cloud patch is expanded slightly and taken as identified cloud shadow. For Landsat ETM+ imagery with scan-line gaps, a majority filter fills scan gaps with clouds or potential cloud shadows where these elements are in the image data surrounding gaps. Final manual refinement was followed by adding a three-pixel buffer to both the clouds and the identified cloud shadows. The buffer removes mixed pixels that occur around cloud edges.

3.4. Collecting reference data on tropical forest association

We used the hierarchical classification system of Beard (1944a, 1946a) who classified native forests in Trinidad and Tobago and mapped their distributions on public lands (which comprise about 40% of the land). The system starts with floristic groups that are "recognizable by diagnostic species." The associations are grouped into alliances of canopy dominants and then into formations based on physiognomic factors, primarily structure, deciduousness, and other characteristics of leaf type (Tables 1 and 2; local names in S1–S2). Formations "express a habitat determined by the interplay of the environmental factors of climate, topography, and soil" (Beard, 1944b, 1946a). Montane seasonal forests, for example, are "seasonal" because of the importance of deciduous species, which are more common in this forest than in other montane forest because it occurs on more freely draining limestone substrates. The associations within a formation, though floristically defined, usually also differ slightly in physiognomy. The semi-evergreen associations differ in deciduousness, for example, as do some of the seasonal evergreen associations. Vegetation physiognomy affects spectral response in satellite imagery, particularly deciduousness and canopy development. It follows that because several floristic associations are physiognomically distinct, they may also be distinct in multispectral imagery if it is dated from the correct season or year.

Beard based his system on strip surveys conducted from 1927–1933 and 1941–1942, and aerial photos from 1938 (scale 1:40,000). All trees >9.9 cm diameter at breast height (dbh) were counted along continuous, 10-m wide transects, and then summed by species over each 200-m long section. The plot networks were dense: transects in central and southern Trinidad, for example, were spaced only 2 km apart, resulting in about 1600 plots.

Given the high spatial density and large number of plots Beard used, and the detailed descriptions and tallies of the species composition and deciduousness of associations, we assumed that this classification system is valid for forests where large-scale clearing for agriculture did not occur since the surveys, even though it was not based on modern ordination techniques. We also assumed that we could rely on the Beard maps as one information source when learning to identify forest classes in fine resolution imagery. Our conclusions are conditioned on these assumptions. Forest associations on public lands were again mapped with aerial photos from 1969 and field work conducted in 1979–1980 (FRIM, 1992), and the mapping results are almost identical. We modified the names

Table 1
Forest classes mapped for Trinidad; mature forest classes are those from Beard (1946a,b).[a]

Forest Formation and Association according to Beard (1946a,b)	Symbol	Identifying sources[a]
Dry evergreen forest–littoral woodland (canopy)		
Coccoloba uvifera–Hippomane mancinella[b]	LWS	1 m Img, Maps, Field[b]
Roystonea oleracea–Manilkara bidentata[b]	LWP	1 m Img, Maps[b]
Deciduous seasonal forest (canopy)		
Machaerium robinifolium–Lonchocarpus punctatus–Bursera simaruba	Ss	1 m Img, Field, L7 200303
Deciduous to semi-evergreen seasonal forest (canopy)		
Protium guianense–Tabebuia serratifolia ecotone and *Peltogyne floribunda–T. serratifolia–P. guianense*	Ip	1 m Img, Field, L7 200303
Semi-evergreen seasonal forest (canopy)		
P. floribunda–Mouriri marshallii	Pbl	Plots, 1 m Img, Maps, Field
Trichilia pleeana–Brosimum alicastrum–Bravaisia integerrima	Aj	Plots, 1 m Img, Maps, Field
T. pleeana–B. alicastrum–Protium insigne	Ag	Plots, 1 m Img, Maps, Field
B. alicastrum–Ficus yoponensis[b]	Af	Maps, L5 1987[b]
Evergreen seasonal forest (emergents/canopy/subcanopy)		
Aniba panurensis and *A. trinitatis-Carapa guianensis/Ligania biglandulosa*	Cd	Maps, Field
A. panurensis and *A. trinitatis – Carapa guianensis – Eschweilera subglandulosa/Pentaclethra macroloba/Attalea maripa*	Cco	Plots, 1 m Img, Maps, Field, L7200301
C. guianensis–Pachira insignis – E. subglandulosa/P. macroloba/Sabal sp.	Cca	Plots, 1 m Img, Maps, Field
E. subglandulosa–P. insignis–C. guianensis/Clathrotropis brachypetala/A. maripa	Cb	Plots, 1 m Img, Maps, Field,
Mora excelsa–C. guianensis/P. macroloba[c]	Cm	Plots, 1 m Img, Maps, Field
Montane rain forest (Canopy)		
Transitional seasonal evergreen to lower montane	Cd-LMF	1 m Img, Maps
Byrsonima spicata–Licania ternatensis–Sterculie pruriens (Lower)	LMF	Maps, Field
Inga macrophylla–Guarea guara (seasonal)[b]	SMF	Maps, L5 1987[b]
Transitional Lower Montane – Montane	LMF-MF	1 m Img, Maps
Richeria grandis–Eschweilera trinitensis (Montane Cloud)	MF	1 m Img, Maps, Field
Forested Wetlands		
Mangrove (includes different associations)[d]	ESM	1 m Img, Maps, Field
Other swamp communities[e]	ESO	1 m Img, Maps, Field
Young secondary forest classes		
Hevea brasiliensis – former plantation	Br	1 m Img, Field, L7200301
Young secondary forest (<15–20 yr)	YSF	1 m Img, Field
Young secondary forest (<35–40 yr) or abandoned or semi-active woody agriculture	YSF-Wag	1 m Img, Field
Young secondary forest – former *Cocos nucifera* plantation	YSF-C	1 m Img, Field
Bambusa vulgaris	YSF-B	1 m Img, Field
Tree plantations		
Tectona grandis[b]	PT	1 m Img, Field[b]
Pinus caribaea[b]	PP	1 m Img, Field[b]
Other[b]	PO	1 m Img, Field[b]

[a] The latin names for seasonal and semi-evergreen forest types are altered to better represent canopy dominance. ¹Plots = Plots; Field = field identification; 1 m Img = ⩽1-m imagery; Maps = Maps from air photos and plots (Beard (1946a,b); FRIM, 1992); L7 = Landsat 7 ETM+; L7 2003 03 = L7 from 03/31/2003; L7 2003 01 = L7 from 01/19/2003; L5 1987 = Landsat 5 TM dated 05/07/1987.

[b] Manually delineated.

[c] Both modeled and manually delineated.

[d] Associations may include these species: *Rhizohpora mangle, R. harrisonii, R. racemosa, Avicennia germinans, A. Schaueriana, Laguncularia racemosa,* or *Conocarpus erectus.*

[e] The Class other swamp communities was manually differentiated, based on ⩽1-m imagery, into palm swamp (*Roystonea oleracea* or *Mauritia flexuosa*), swamp forest (*Pterocarpus officinalis*); swamp forest ecotone (*Carapa guianensis–Ptercarpus officinalis*), marsh forest (*Manicaria saccifera–Jessenia oligocarpa–Euterpe precatoria*), or marsh forest – seasonal evergreen ecotone.

of evergreen seasonal associations, adding other diagnostic dominant species that Beard mentions in addition to the timber species.

Data for training and testing the classification models came from assigning land cover or forest type to patches of about 16 or fewer pixels (but only one to four pixels for low-density urban lands). The data sources were: (1) three weeks of field work in which experts identified forest association in locations throughout the islands; (2) the locations of 241 inventory plots that experts had labeled to forest association; and 3) learning to identify many of the forest associations in fine resolution imagery (or in two cases in Landsat imagery), based on the field work, plots, and unique historical work by Beard (1944a, 1946a). The large number of Beard's associations that we could identify was unexpected, and we give more details in the results section.

Fine resolution imagery (⩽1 m) was available for the entire study area and dated from October 2000 to August 2009. Most data was from 2004 to 2007. It included island-wide tiled mosaics of

pan-sharpened, true color IKONOS images (examples shown in S3); island-wide tiled mosaics of black-and-white, orthorectified digital air photos; and pan-sharpened, true color images from Digital Globe that were viewable with Google Earth. The Google Earth images included most of the IKONOS images above, but also included more than one date of fine resolution imagery for most places.

Two or more distinct spectral classes were discernible for some forest types. We separated such classes in decision-tree models and then recombined them in the final map and accuracy assessment. For example, a gradient of decreasing greenness from west to east was evident for two of the lowland seasonal evergreen associations. This gradient likely reflects the gradient of increasing deciduousness that Beard (1946a) mentions. As in prior work, a sunlit and shadowed spectral class represented each forest type in hilly areas. We also separated the training pixels for Mora forests into three geographic regions: south, central and Northern Range.

Table 2

Forest classes mapped for Tobago; mature forest classes are those from Beard (1944a,b).

Forest formation and association	Code	Identifying sources[a]
Dry evergreen forest – littoral woodland		
Coccoloba uvifera–Hippomane mancinella[b] _Manilkara bidentata_[b]	LWS[b] XFBa[b]	1 m Img, Maps, Field 1 m Img, L72000 08
Deciduous seasonal forest		
Bursera simaruba–Coccothrinax barbadensis	Ssd	1 m Img, Maps, Field
Semi-evergreen seasonal forest		
Hura crepitans–Tabebuia chrysantha–Spondias mombin	Sch	1 m Img, Maps, Field
Lowland rain forest		
Carapa guianensis–Euterpe precatoria	Ccp	1 m Img, Maps, Field
Xerophytic rain forest		
Manilkara bidentata–Guettarda scabra	XFBb	1 m Img, Maps, L72000 08
Lower montane rain forest		
Licania biglandulosa – Byrsonima spicata	LMF	1 m Img, Maps, Field
Young secondary forest classes		
Young secondary forest (<15-20 yr), abandoned woody agriculture	YSF-Wag	1 m Img, Field
Secondary forest – former _Cocus nucifera_ plantation[b]	YSF-C[b]	1 m Img, Field
Bambusa vulgaris	YSF-B	1 m Img, Field
Forested wetlands		
Mangrove	ESM	1 m Img, Maps, Field
Other wooded wetlands	ESO	1 m Img, Maps, Field

[a] Field = field identification; 1 m Img = ⩽1-m imagery; Maps = maps from air photos and plot data (Beard (1944a,b)) and maps, air photos and fieldwork from FRIM (1992); L72000 = Landsat 7 ETM+, 001/052, dated 08/06/2000.

[b] Manually delineated.

Table 3

Four gap-filled Landsat image mosaics were created for Trinidad and one for Tobago from the 19 scenes listed here. Each mosaic included a reference, or _base_ scene. The clear parts from other scene dates, or _fill_ scenes, then filled the cloudy parts of the base scene after undergoing normalization to the base scene with the regression tree method of Helmer and Ruefenacht (2005). Fill scenes are listed in the order that they filled cloudy areas in the base scene (_i.e._, top to bottom). Scene types: L5 = Landsat 5 TM; L7 = Landsat 7 Enhanced TM.

Dates and types of scenes in gap-filled mosaics (month/day/year)	Percent of studyarea	Dates and types of scenes in gap-filled mosaics (month/day/year)	Percent of study area
Trinidad 2007, path/row 233/053		_Trinidad 1980s, path/row 233/053_	
12/16/2007 – L7	57	03/14/1985 – L5	46
03/05/2002 – L7	21	05/04/1986 – L5	22
01/29/2001 – L7	13	05/07/1987 – L5	10
04/17/2006 – L7	3.3		
01/30/2007 – L7	1.5	05/04/1986 – L5	42
03/21/2008 – L7	0.7	03/14/1985 – L5	27
02/03/2006 – L7, 001/053	1.3	05/07/1987 – L5	10
02/11/2003 – L7, 001/053	1.4		
01/24/2008 – L7	0.02	05/07/1987 – L5	34
10/25/2000 – L7	0.3	03/14/1985 – L5	29
		05/04/1986 – L5	14
Tobago 2007, path/row 233/052			
12/16/2007 – L7	63		
12/02/2008 – L7	14		
02/18/2008 – L7	5.7		
02/02/2008 – L7	6.0		
04/01/2006 – L7	6.2		
11/13/2001 – L7	3.9		

3.5. Classifications and classification comparisons

To create classification mapping models, we applied the decision-tree software See5 to text files that list class assignment and values for spectral and ancillary _predictor layers_ for each reference pixel. To produce each map, we applied the models from See5 to the stack of spectral and ancillary data layers with software from Ruefenacht et al. (2008).

A randomly-selected 90% of the reference data served to train each classification model, leaving 10% of the data for estimating model error. On average, then, about one to two pixels per patch were available for testing. Calculating classification accuracy from pixels that are randomly selected from multi-pixel patches of training data likely yields optimistic error estimates. The bias

arises because pixels within a patch are likely to be more similar to each other than to other pixels of the same class. Limiting test data to 10% of the reference data reduces this bias from the more commonly withheld proportion of 30%, but probably does not remove it. Sufficient resources were not available for a completely independent accuracy assessment (Sesnie et al., 2008).

We used one decision-tree classification model to simultaneously map both land cover and forest type for Tobago, as Tobago has only seven main forest associations that are closely related to topography. The model used the gap-filled image centered on 2007 and the other predictor layers listed in the next section.

Trinidad was divided into two mapping zones: the Northern Range was one; the rest of Trinidad (the "lowlands") was the other. With the decision-tree software described above, we first mapped

land cover for the two Trinidad zones with the gap-filled image centered on 2007. We then mapped forest type for the two Trinidad zones for the areas that the land-cover models classified as forest, using the gap-filled imagery centered on 2007, all three of the gap-filled images from the 1980s, and the other predictor layers described below. In those results Mora forests in the southeast and Northern Range showed more confusion with other forest types. Consequently, we manually cleaned up the result for Mora forests in those areas and then overlaid the edited Mora forests onto forest types as mapped after excluding Mora training points in those areas.

To test if the gap-filled imagery from the 1980s and the thermal band improved classifications, we compared overall accuracy, class-specific accuracies, and the Kappa coefficient of agreement of models that used various band combinations. We tested whether overall and class-specific accuracies differed significantly via the McNemar test for comparing related proportions (Foody, 2009). Comparisons were of (1) land cover with *vs.* without the gap-filled thermal band; and (2) for Trinidad, forest association with *vs.* without one or more of the gap-filled images from the 1980s.

3.6. Ancillary environmental predictor layers

We considered the following predictor layers for the decision-tree classification models: spectral bands and indices from the gap-filled imagery; maps of rainfall and temperature (Hijmans et al., 2005); and topography (Farr et al., 2007), geology (Suter, 1960; Snoke et al., 2001b) and geographic position. Hijmans et al. (2005) mapped climate at 1-km resolution based on climate station data and topography. Their data did not include the denser network of rain gauges set up by the local water authority, but those rainfall data were not available to us. Topographic layers included elevation, slope, slope position, curvature, sine and cosine of aspect, topographic shading for the time of the base scene for

each gap-filled image, and topographic relative moisture index (TRMIM) (Manis et al., 2002). We used these topographic derivatives to represent soil drainage.

Spectral data included all bands from each Landsat mosaic, a date band (*e.g.* Fig. 2a and c) and six spectral indices. The indices were tasseled cap (TC) brightness, greenness and wetness (Crist and Cicone, 1984; Huang et al., 2002), the wetness–brightness difference index (WBDI) (Helmer et al., 2009), the normalized difference vegetation index (NDVI), and the normalized difference structure index (NDSI) (Hardisky et al., 1983; Helmer et al., 2010):

$$WBDI = TC\ Wetness - TC\ Brightness \tag{1}$$
$$NDVI = (NIR_{b4} - RED_{b3})/(NIR_{b4} + RED_{b3}) \tag{2}$$
$$NDSI = (NIR_{b4} - SWIR_{b5})/(NIR_{b4} + SWIR_{b5}) \tag{3}$$

3.7. Manual delineation and editing

Several forest associations were manually delineated (Tables 1 and 2). We manually delineated managed and former timber plantations, including teak, Caribbean pine and abandoned Brazilian rubber. Though usually spectrally distinct from adjacent forest, delineating them was fast, thanks to their regular boundaries and limited number, and would reduce confusion among other classes. Spanish cedar plantations are also common in Trinidad. Though we located many patches of it during field work, most of them were too small to be clearly identifiable in the Landsat imagery. We also manually delineated the two littoral forest associations. Many of the patches were narrow, resulting in pixels being mixed with water, sand or wetland, making their spectral signatures highly variable. Nonforested wetlands were also manually delineated due to large signature variability. Nonmangrove forested wetlands were one class in decision-tree models and then manually divided into subclasses. Most other manual editing corrected confusion between Mora forests and other seasonal evergreen associations, or
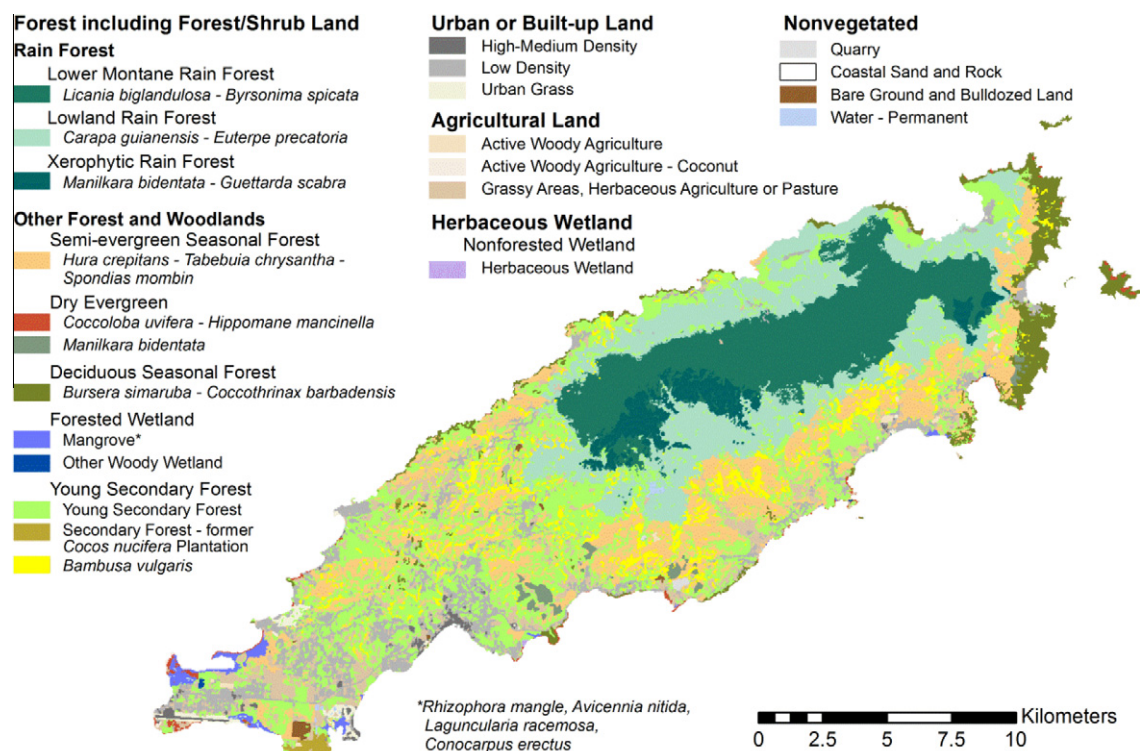

Fig. 3. Forest association and land cover for Tobago were mapped with decision-tree classification of gap-filled Landsat 7 imagery centered on December 2007. Mature forest associations are classified according to the system of Beard (1944).
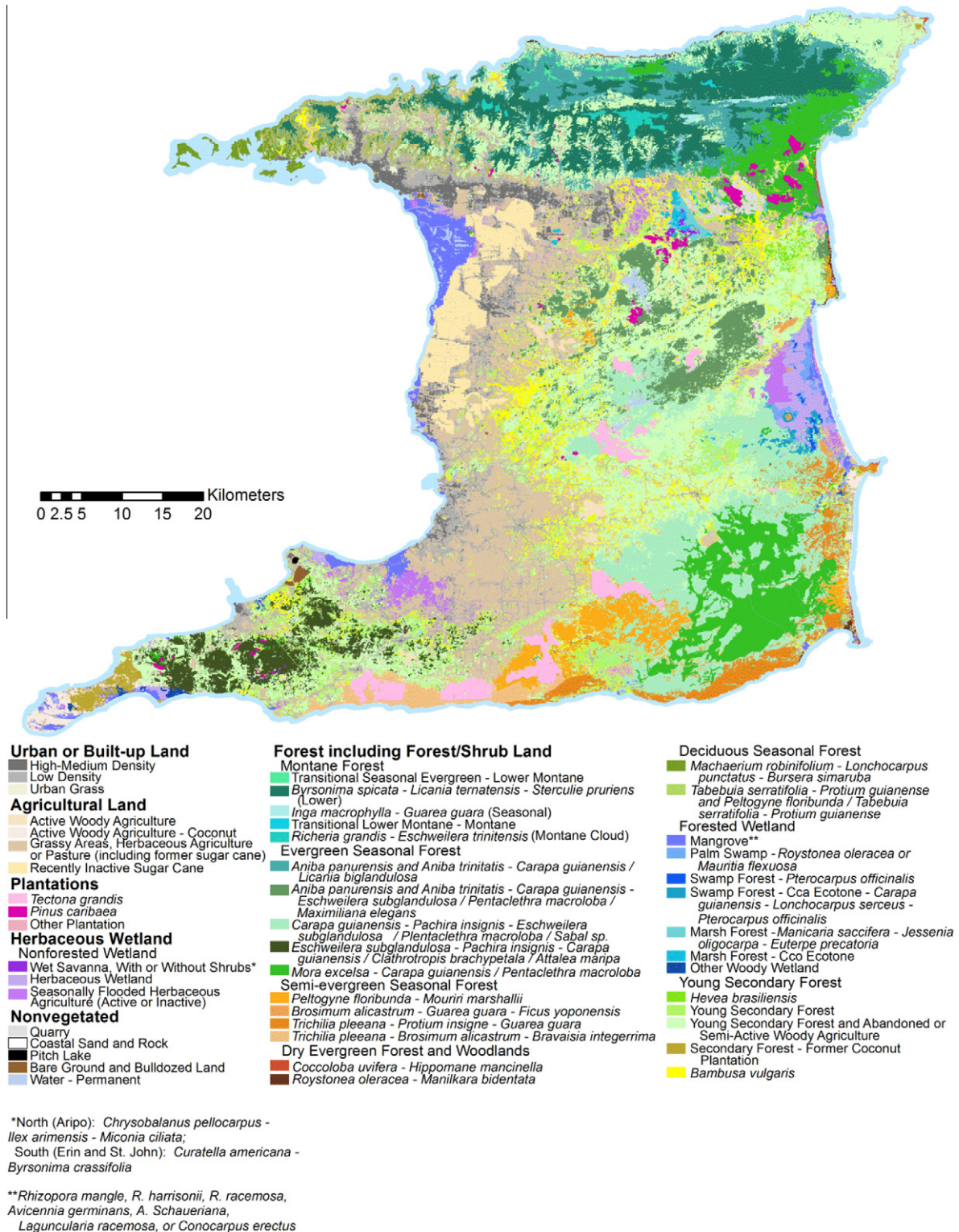
Urban or Built-up Land
High-Medium Density
Low Density
Urban Grass

Agricultural Land
Active Woody Agriculture
Active Woody Agriculture - Coconut
Grassy Areas, Herbaceous Agriculture or Pasture (including former sugar cane)
Recently Inactive Sugar Cane

Plantations
Tectona grandis
Pinus caribaea
Other Plantation

Herbaceous Wetland
Nonforested Wetland
Wet Savanna, With or Without Shrubs*
Herbaceous Wetland
Seasonally Flooded Herbaceous Agriculture (Active or Inactive)

Nonvegetated
Quarry
Coastal Sand and Rock
Pitch Lake
Bare Ground and Bulldozed Land
Water - Permanent

Forest including Forest/Shrub Land
Montane Forest
Transitional Seasonal Evergreen - Lower Montane
Byrsonima spicata - Licania ternatensis - Sterculie pruriens (Lower)
Inga macrophylla - Guarea guara (Seasonal)
Transitional Lower Montane - Montane
Richeria grandis - Eschweilera trinitensis (Montane Cloud)
Evergreen Seasonal Forest
Aniba panurensis and Aniba trinitatis - Carapa guianensis / Licania biglandulosa
Aniba panurensis and Aniba trinitatis - Carapa guianensis - Eschweilera subglandulosa / Pentaclethra macroloba / Maximiliana elegans
Carapa guianensis - Pachira insignis - Eschweilera subglandulosa / Plentaclethra macroloba / Sabal sp.
Eschweilera subglandulosa - Pachira insignis - Carapa guianensis / Clathrotropis brachypetala / Attalea maripa
Mora excelsa - Carapa guianensis / Pentaclethra macroloba
Semi-evergreen Seasonal Forest
Peltogyne floribunda - Mouriri marshallii
Brosimum alicastrum - Guarea guara - Ficus yoponensis
Trichilia pleeana - Protium insigne - Guarea guara
Trichilia pleeana - Brosimum alicastrum - Bravaisia integerrima
Dry Evergreen Forest and Woodlands
Coccoloba uvifera - Hippomane mancinella
Roystonea oleracea - Manilkara bidentata

Deciduous Seasonal Forest
Machaerium robinifolium - Lonchocarpus punctatus - Bursera simaruba
Tabebuia serratifolia - Protium guianense and Peltogyne floribunda / Tabebuia serratifolia - Protium guianense
Forested Wetland
Mangrove**
Palm Swamp - *Roystonea oleracea or Mauritia flexuosa*
Swamp Forest - *Pterocarpus officinalis*
Swamp Forest - Cca Ecotone - *Carapa guianensis - Lonchocarpus serceus - Pterocarpus officinalis*
Marsh Forest -*Manicaria saccifera - Jessenia oligocarpa - Euterpe precatoria*
Marsh Forest - Cco Ecotone
Other Woody Wetland
Young Secondary Forest
Hevea brasiliensis
Young Secondary Forest
Young Secondary Forest and Abandoned or Semi-Active Woody Agriculture
Secondary Forest - Former Coconut Plantation
Bambusa vulgaris

*North (Aripo): *Chrysobalanus pellocarpus - Ilex arimensis - Miconia ciliata;*
South (Erin and St. John): *Curatella americana - Byrsonima crassifolia*

**Rhizopora mangle, R. harrisonii, R. racemosa, Avicennia germinans, A. Schaueriana, Laguncularia racemosa, or Conocarpus erectus*

Fig. 4. Before mapping forest association, land cover was mapped for Trinidad with decision-tree classification of gap-filled Landsat 7 imagery centered on December 2007, which is the early dry season. Forest association was then mapped for those areas classified as forest with the gap-filled imagery from 2007 plus three gap-filled images from the 1980s that were from the mid to late dry season. Mature forest associations are classified according to the system of Beard (1946a).

corrected scattered pixels of agriculture that were misclassified as urban lands.

4. Results

The final map of land cover and forest associations for Tobago (Fig. 3) included the most accurate overall classification, which in-

cluded the thermal band. The final map for Trinidad (Fig. 4) combined the most accurate land-cover classification, which included the thermal band, the most accurate classifications of forest association, which included all of the gap-filled images from the 1980s, and the edited Mora forests (Fig. 5). Where residual gaps existed in the 1980s gap-filled imagery, forest association was mapped with only the 2007 gap-filled image.
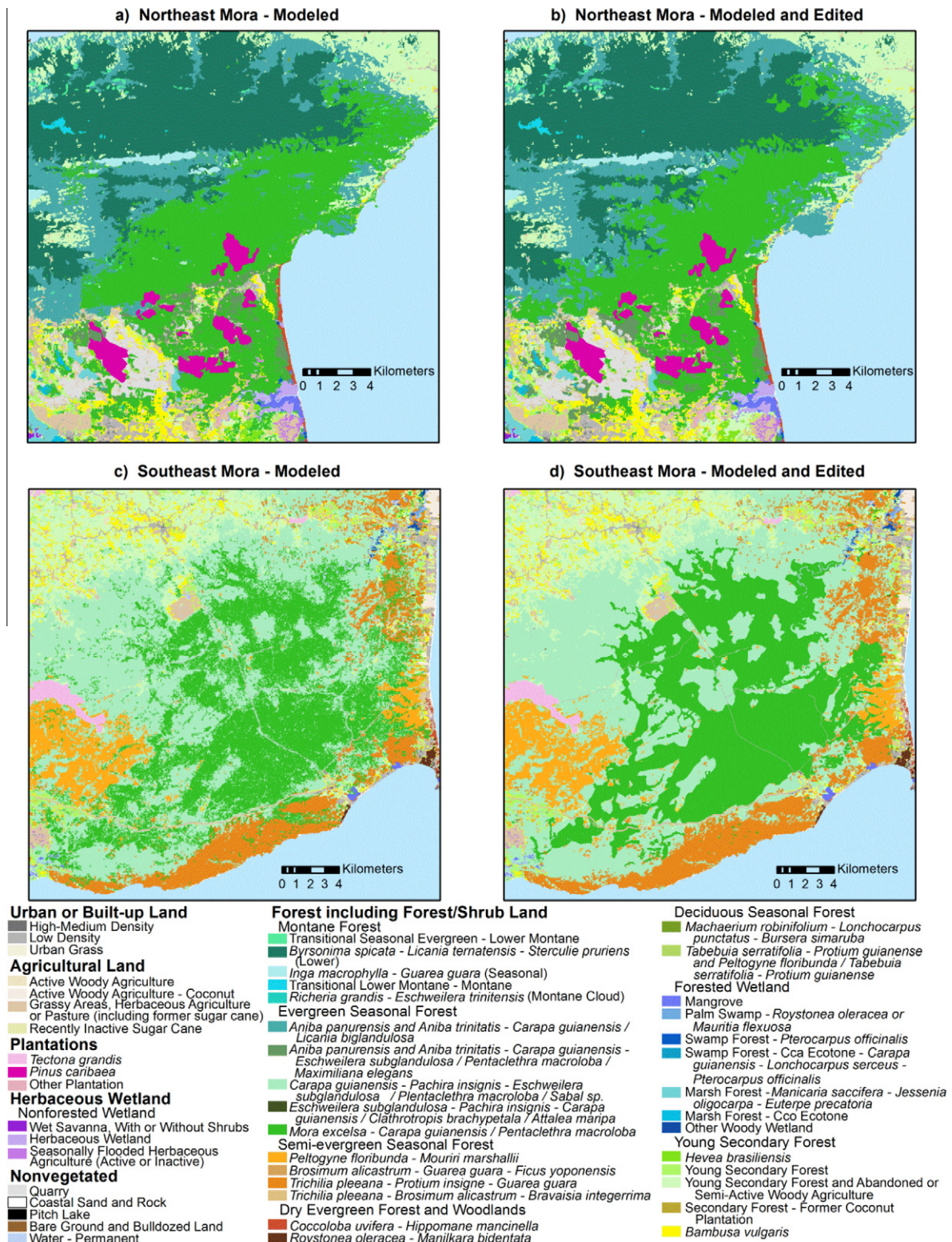
Fig. 5. Modeled *vs.* modeled and edited distribution of *Mora excelsa* forests in the Northern Range (a and b) and in the southeastern lowlands (c and d) of Trinidad.

4.1. Interpreting forest association in fine resolution and multiseason imagery including Google Earth

In supplementing field data with classification training data collected from the fine resolution imagery, unique canopy structure distinguished nine associations, plus mangroves, regardless of season. For example, one littoral association has frequent palms; the other has prostrate stems on the windward edges of patches, which are narrow. Also with distinct canopy structure were swamp forest (*Pterocarpus officinalis*), palm swamp, *Mora excelsa* forests (Cm), bamboo stands (*Bambusa vulgaris*), abandoned coconut (*Cocos nucifera*), teak (*Tectona grandis*) and pine (*Pinus caribaea*).

Apparent differences in water level also helped distinguish forested wetlands from other forests. *Mora excelsa* forests, which are a monodominant type, have a smoother canopy that is 15 m taller and has larger crowns than adjacent types (S3-a). Beard could distinguish this association in air photos.

For an additional seven associations, plus abandoned woody agriculture, we identified unique canopy features that were only present in certain seasons or dates of the fine resolution imagery. Two or more fine resolution images were available for nearly all of the study area. Images displaying the seasonal image elements

that identified association were available for at least half of the extent of the seven associations. Examples of these elements are the lowland seasonal evergreen association Cco, which has a canopy punctuated by dark crowns in scenes from late April (S3-b), probably the result of flushing leaves which can be red to brown in color, distinguishing it from another lowland seasonal evergreen type (Cca). The same dark crowns distinguished the two seasonal evergreen associations of the Northern Range (Cd and transitional Cd) from types at higher elevations. Differences in relative deciduousness showed distinct boundaries between three lowland semi-

Table 4
Overall and class-specific overall accuracy for Tobago classification of land cover and forest type. The relative differences in bold typeface are significant at $p < 0.05$.

| Forest formation and association	Code	Excluding thermal	Including thermal	Relative difference (%)
Kappa coefficient of agreement		0.93 ± 0.01	0.93 ± 0.01	
Overall accuracy (%)		94	94	0
Dry evergreen forest – littoral woodland				
Coccoloba uvifera–Hippomane mancinella	LWS	64	72	13
Deciduous seasonal forest				
Bursera simaruba–Coccothrinax barbadensis	Ssd	98	98	0
Semi-evergreen seasonal forest				
Hura crepitans–Tabebuia chrysantha–Spondias mombin	Sch	90	91	1
Xerophytic rain forest				
Manilkara bidentata–Guettarda scabra	XFBb	91	93	2
Lowland rain forest				
Carapa guianensis–Euterpe precatoria	Ccp	94	92	**−2**
Lower montane rain forest				
Licania biglandulosa–Byrsonima spicata	LMF	96	96	0
Young secondary forest classes				
Young secondary forest (<15-20 yr)	YSF-Wag	89	89	0
Bambusa vulgaris	YSF-B	79	79	0
Edaphic swamp communities				
Mangrove	ESM	96	96	0
Other wooded wetlands	ESO	86	86	0
Nonforest classes				
Herbaceous agriculture		73	93	**27**
Water		100	100	0
Urban, high density		94	94	0
Urban, low density		91	88	−3
Grassy areas, pasture		97	96	−1
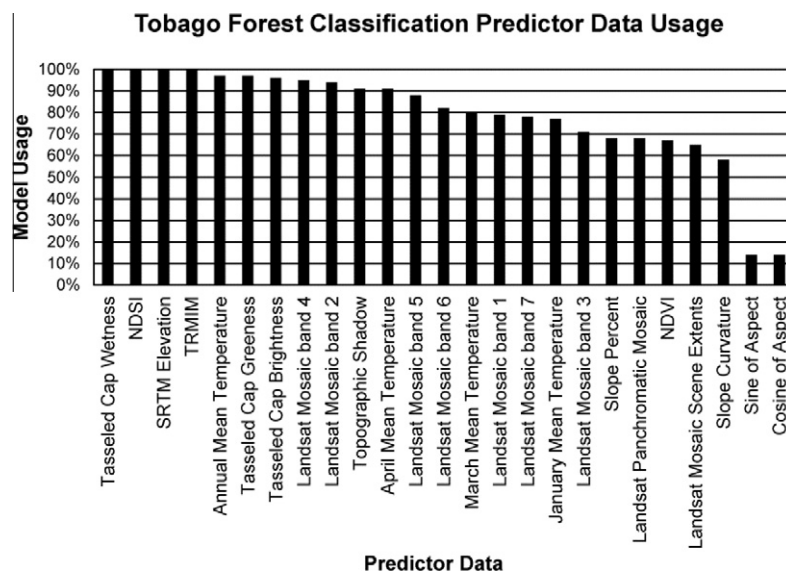
Fig. 6. For the Tobago classification model, the percentage of cases in which the indicated layer was used in at least one classification rule.

evergreen associations (Pbl, Aj and Ag). Based on deciduousness we could also distinguish seasonal from semi-evergreen associations, including in an area that Beard maps a mixture of the two (Cca vs. Ag). The semi-evergreen association is either more deciduous or a brighter green (caused by leaf flush of deciduous species) than the seasonal evergreen one (Fig. S3-c). Abandoned woody agriculture was also distinct in fine resolution imagery if *Erithryna poeppigiana* was in bloom. It is a nitrogen-fixing legume with conspicuous coral-colored flowers that farmers plant to shade and fertilize coffee or cocoa (Fig. S3-d). This feature was mainly present in the Northern Range.

Although the boundaries between many associations were sharp, some of the forest to which we assign a community type is no doubt transitional between two community types. In these cases we assigned type based on whether the available dates of fine resolution imagery displayed the identifying deciduousness or other canopy features described above. One example area is the south central lowlands where two large patches we map as predominantly a seasonal evergreen type (Cca) may be transitional with the nearby semi-evergreen type of Pbl. Another example is in the central lowlands where, based on deciduousness, we assign Ag to scattered patches that occur on small hills where the matrix is
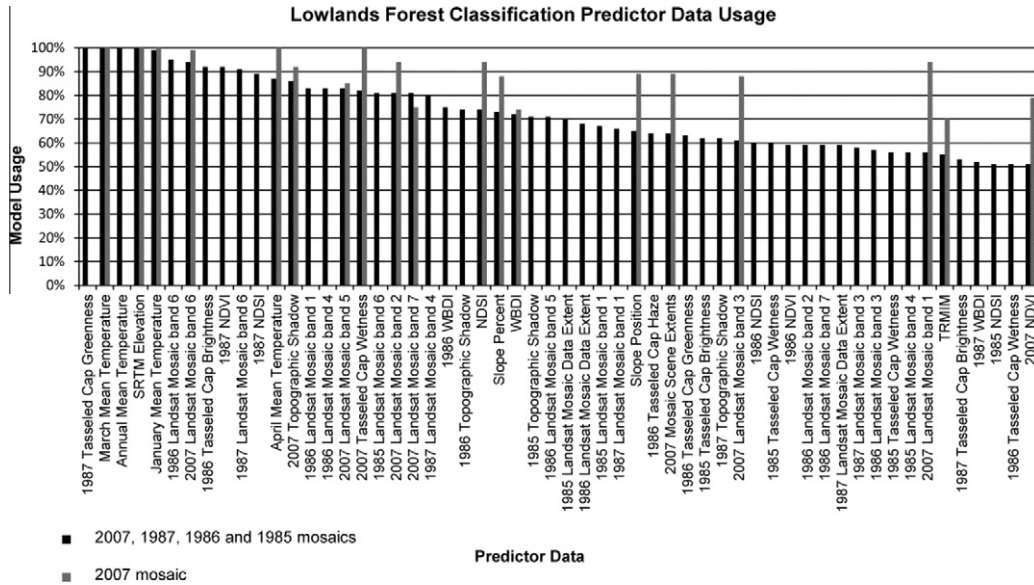

Fig. 7. The percentage of cases in which the indicated layer was used in at least one classification rule for forest type mapping of the Trinidad lowlands. The lighter bars indicate attribute usage for classifications using the three 1980s gap-filled images in addition to the 2007 gap-filled image. The darker bars indicate attribute usage for the classification model that used only the 2007 gap-filled image.
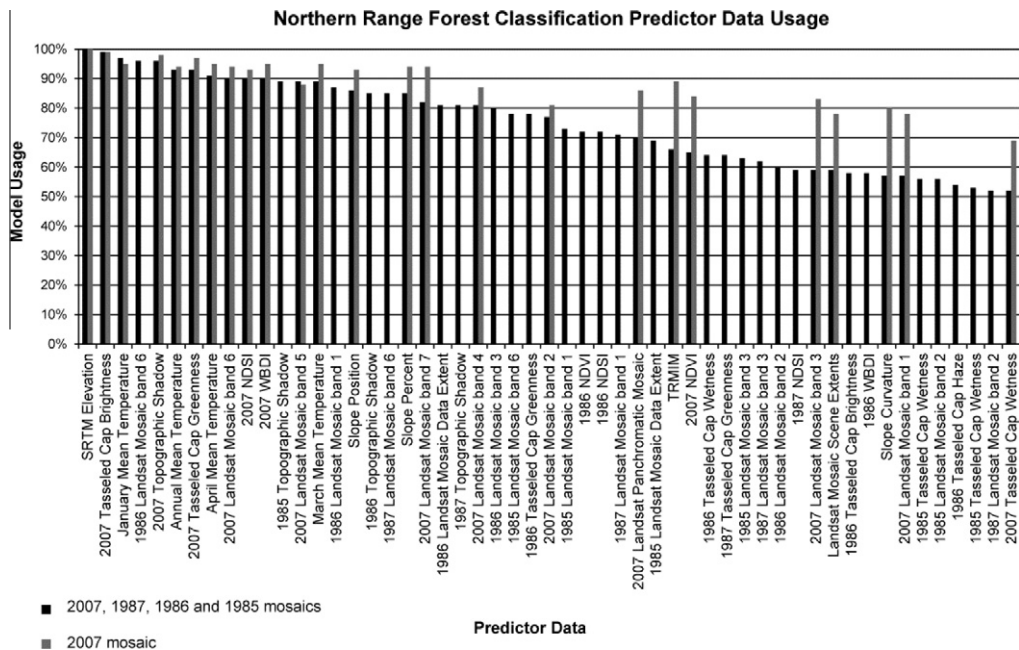

Fig. 8. For forest type mapping of the Trinidad Northern Range mapping zone, the percentage of cases in which the indicated layer was used in at least one classification rule. The lighter bars indicate attribute usage for classifications using the three 1980s gap-filled images in addition to the 2007 gap-filled image. The darker bars indicate attribute usage for the classification model that used only the 2007 gap-filled image.

Table 5

A comparison of overall accuracies for Trinidad, including class-level accuracies. Decision tree classification models that include the gap-filled image from 2007, but that exclude one to three of the 1980s gap-filled images, are compared against models that include all of the gap-filled images (N = 8525 for Trinidad's lowlands and 8757 for the rest of Trinidad). In the Lowlands, the most accurate models used at least two of the gap-filled images from the 1980s, particularly those representing the driest conditions.

Overall accuracy (%) and significance of difference from base case of including all 1980s imagery[c]							
	No. 1980s	1985	1986	1987	1985, 86	1985, 87	1986, 87	Base case All 1980s
Synthetic multiseason images included with 2007 image [a] – Trinidad lowlands								
Kappa statistic[b]	0.84	0.88	0.89	0.90	0.90	0.90	0.91	0.92
Overall	86[***]	90[***]	91[***]	91[***]	91[***]	92[**]	93	93
Semi-evergreen seasonal forest								
Pbl	77[***]	87[*]	86[**]	89	88[*]	91	90	91
Aj	80[***]	92	87[***]	95	91[*]	96	93[*]	96
Ag	82[***]	86[***]	88[*]	91	91	95	92	93
Ag_2	59[***]	73[***]	82	76[*]	82	77[*]	82	83
Evergreen seasonal forest								
Cco	88[**]	89[*]	91	91	91	90[*]	92	93
Cca	89[***]	92[**]	92[**]	92[**]	92[**]	93[*]	93	94
Cb	85[**]	89[*]	93	91	93	91	94	93
Cm	92	94	97	95	95	93	97	95
Young secondary forests								
YSF	82	88	88	92	84	84	88	87
YSF-Woody Ag	85[*]	86	87	88	88	89	91	89
YSF-Bamboo	90	92	93	91	94	94	94	93
Forested wetlands								
Mangrove	99	100	100	99	100	100	99	99
Inland Swamp	93	95	98	95	96	97	95	97
Synthetic multiseason images included with 2007 Image[a] – Trinidad Northern Range								
Kappa statistic[b]	0.89	0.90	0.91	0.91	0.91	0.91	0.91	0.91
Overall	93[**]	94	94	94	94	94	94	94
Deciduous to semi-evergreen seasonal forest								
Ip, Ss	74[**]	86	90	87	93	88	90	88
Evergreen seasonal forest								
Cd	99	99	99	99	99	99	99	99
Montane rain forest								
Cd_LMF	63	64	68	70	69	68	71	65
LMF	94	95	95	95	95	94	95	95
MF	94	95	93	93	95	95	94	94
Young secondary forests								
YSF-Woody Ag	77[*]	79	79	80	80	81	84	83
YSF-Bamboo	98	98	100	100	100	98	100	100

[a] *No 1980s* = all 1980s mosaics excluded; *1985* = the only mosaic included with the 2007 mosaic is that with the reference scene from 1985; *1985, 86* = image mosaics with the reference scenes from 1985 and 1986 are included with the mosaic from 2007, *etc.*
[b] The 95% confidence interval for all Kappa estimates rounds to ±0.01; differences between Kappa estimates that are larger than ±0.01 are significant at $p < 0.05$.
[c] McNemar test for related proportions.
[*] $p < 0.05$.
[**] $p < 0.005$.
[***] $p < 0.0005$.

Cca. These patches likely receive more rainfall than the Ag patches closer to the coast. They are likely transitional between the Ag and Cca communities.

An additional four associations have distinct boundaries in particular Landsat image dates (Tables 1 and 2), two of which we manually digitized from specific scenes (SMF and Br). Tobago's xerophytic rain forest (XfBb) displayed a larger band 4:5 ratio in wet-season imagery, which we have observed occurs in other Caribbean forest types with hard leaves and a wind-clipped canopy, though we have not seen this observation mentioned elsewhere. Other examples were distinct in a specific image date (Table 1) because of a leaf-off condition, including the distinction between deciduous and semi-evergreen forests on the Chaguaramas Peninsula in northwest Trinidad (Ss *vs.* Ip); former plantations of Brazilian rubber (*Hevea brasiliensis*); and the main areas of the montane seasonal forest (SMF). In these images these forest associations reflected more light in the red band and less in the near infrared band as compared with adjacent forest. The image from the 1987 drought was the only image we found in which montane seasonal forests, which are more seasonal because they occur on

more freely draining limestone substrates, had dropped so much foliage as to be distinct from surrounding forest. Another note is that strategic display of Landsat bands 7, 2 and the wetness–brightness difference index (WBDI) revealed the extent of lowland Mora. In this display it appears greener on flat lands than other old-growth forest because it tends to be brighter in the visible band 2, possibly because its monodominant and therefore smoother canopy has less shadow.

4.2. Classification models

4.2.1. Land-cover classifications and the influence of the thermal band

In Tobago (Fig. 3), the test data for land cover and forest association were classified with an overall accuracy of 94% (Table 4). Class-specific accuracies for test data on forest associations ranged from 72% to 98% (Table 4). Though we did not make multiseason image mosaics for Tobago, it has fewer associations, most of which are closely related to topography. The land-cover classification models for the Northern Range and lowlands of Trinidad (Fig. 4)

both classified 97% of test pixels correctly. Test data for all land-cover types were classified with at least 90% overall accuracy.

Including the thermal band in the Tobago classification significantly increased model accuracy for herbaceous agriculture by 27% ($p < 0.05$), mainly by reducing confusion with urban grass, but it lowered accuracy for classifying Lowland Rain Forest by 2% (Table 4). The thermal band slightly improved overall accuracy for classifying urban lands in the Northern Range of Trinidad, in this case for high density urban lands (by 4%, $p < 0.005$).

4.2.2. Environmental predictors of forest association

Of the nonspectral predictor layers, temperature variables, elevation, and topographic shadow were included in the most rules of the decision-tree classification models (Figs. 6–8). Initial tests caused us to exclude geographic position (with one exception), rainfall and geology from the mapping model predictor layers, even though they are highly predictive of forest type. Despite steps to avoid overfitting, patterns in mapped forest types corresponded more closely to rainfall or geology than to their actual distributions (based on comparisons with the fine resolution imagery or other reference data). This outcome was problematic because the rainfall maps, for example, lacked sufficient spatial detail to capture the actual distributions of forest types. Steps to avoid overfitting included trials with different levels of tree pruning, which removes parts of trees, and different minimum numbers of training cases

for each branch. The exception for geographic position was that it improved mapping of *Mora excelsa* forests in the Northern Range (within the seasonal evergreen group, the Mora forests are the medium green patches in the northeast and southeast part of Trinidad). Mora is dispersal limited and otherwise has broad environmental tolerances (Beard, 1946b). Geographic position helped map Mora in the Northern Range because the Mora forests there occur mainly as two large contiguous areas.

Though we removed geology from the sets of predictor layers, we discovered that the spatial distributions of Tobago's "xerophytic rain forest," and that of ultramafic geology in Snoke et al. (2001b), closely correspond. Further, the common dunites among the ultramafic rocks are highly serpentized (Scott et al., 1999). The green, sandy, freely draining soils that Beard (1944a) thought partly responsible for the xerophytism are apparently formed over ultramafic rocks. The forest also shares physiognomic characteristics and many species with Puerto Rican forests formed over ultramafic, serpentine substrate, being dominated by species with shedding bark or evergreen, cutinized leaves. In the wet serpentine forests of Puerto Rico, for example, the trees are "almost all evergreen and sclerophyllous, giving the impression of an anomalous wet desert or dry rain forest" (Ewel and Whitmore, 1973). In Puerto Rico, the forests in these areas include several endemic plant species (Cedeño-Maldonado and Breckon, 1996). Because endemic plants are often found on serpentine substrates, including in the

Table 6

The percentage increase in class-level overall accuracy of decision tree classification models that include 1980s mosaics relative to the base case of models that rely only on the 2007 mosaic. Bold relative difference indicates overall accuracy significantly different from base case at $p < 0.05$.

	Overall Accuracy (%)	Relative Change in Overall Accuracy (%) from Base Case of Excluding 1980s Imagery[a]						
	Base case No 1980s	1985	1986	1987	1985, 86	1985, 87	1986, 87	All 1980s
Synthetic multiseason images added to base case – Trinidad Lowlands								
Semi-evergreen seasonal forest								
Pbl	77	**11**	**10**	13	12	15	14	18
Aj	80	**13**	**8**	**16**	12	17	15	**19**
Ag	82	5	**7**	**10**	10	13	11	**8**
Ag_2	59	**19**	**28**	22	28	22	27	**36**
Evergreen seasonal forest								
Cco	88	2	**3**	**3**	**3**	2	**5**	**4**
Cca	89	**3**	**3**	3	**3**	4	**5**	0
Cb	85	4	**8**	6	**8**	6	**9**	7
Cm	92	3	**5**	**3**	3	1	**5**	**2**
Young secondary forests								
Ysf	82	6	6	**11**	2	2	6	5
Ysf_wag	85	1	2	3	3	4	**6**	5
Bamboo	90	2	3	1	4	4	4	0
Forested wetlands								
Mangrove	99	0	0	0	0	0	0	0
Inland Swamp	93	1	**5**	1	3	4	1	4
	Base 2007 image No. 1980s							
Synthetic multiseason images added to base case[a]–Northern Range								
Deciduous to semi-evergreen seasonal forest								
Ip, Ss	74	**14**	**18**	**15**	**21**	**16**	**18**	**19**
Evergreen seasonal forest								
Cd	99	0	0	0	0	0	0	0
Montane rain forest								
Cd_LMF	63	2	7	10	9	7	**12**	4
LMF	94	0	1	0	1	0	0	0
MF	94	1	−1	−1	1	1	0	0
Young secondary forests								
Bamboo	98	0	2	2	2	0	2	2
Ysf_wag	77	3	3	5	5	5	**9**	**8**

[a] *No 1980s* = all 1980s mosaics excluded; *1985* = the only mosaic included with the 2007 mosaic is that with the reference scene from 1985; *1985, 86* = image mosaics with the reference scenes from 1985 and 1986 are included with the mosaic from 2007, *etc.*

[b] Percentage increase calculated as $(p1 − p2 * 100)/p1$, where $p1$ is the overall accuracy from the left-most column, in which no mosaics from the 1980s mosaics are included with the 2007 mosaic, and $p2$ is the overall accuracy from Table 5 of models that include one or more of the 1980s mosaics together with the mosaic from 2007.

Table 7
Areas of land cover and forest type for Trinidad.

Symbol	Trinidad forest type and land cover	Area (ha)	Percent of Trinidad	Percent of Forest
	Dry evergreen forest–littoral woodland and forest (canopy)	822	0.2	0.2
LWS	*Coccoloba uvifera–Hippomane mancinella*	427	0.1	
LWP	*Roystonea oleracea–Manilkara bidentata*	395	0.1	
	Deciduous to semi-evergreen seasonal forest (canopy)	9617	2.0	2.8
Ss	*Machaerium robinifolium–Lonchocarpus punctatus–Bursera simaruba*	2530	0.5	
Ip	*Protium guianense–Tabebuia serratifolia ecotone and Peltogyne floribunda–T. serratifolia–P. guianense*	7087	1.5	
	Semi-evergreen seasonal forest (canopy)	24,331	5.2	7.1
Pbl	*P.floribunda–Mouriri marshallii*	10,141	2.1	
Af	*Trichilia pleeana–Brosimum alicastrum–Bravaisia integerrima*	481	0.1	
Ag	*T. pleeana–B. alicastrum–Protium insigne*	9293	1.9	
Aj	*B. alicastrum–Ficus yoponensis*	4416	0.9	
	Evergreen seasonal forest (emergents/canopy/subcanopy)	125,024	26.5	36.5
Cd	*Aniba spp.-Carapa guianensis/Ligania biglandulosa (Cd)*	19,947	4.1	
Cco	*Aniba spp.-C. guianensis-Eschweilera subglandulosa/Pentaclethra macroloba/Attalea maripa*	19,232	4	
Cca	*Carapa guianensis-Pachira insignis-E. subglandulosa/P. macroloba/Sabal sp.*	40,230	8.3	
Cb	*E. subglandulosa–P. insignis-C. guianensis/Clathrotropis brachypetala/A. maripa*	12,326	2.6	
Cm	*M. excelsa-C. guianensis/P. macroloba*	33,289	6.9	
	Montane rain forest (canopy)	34,763	7.4	10.2
Cd-LMF	*Transitional seasonal evergreen to lower montane*	1032	0.2	
LMF	*Byrsonima spicata–Licania ternatensis–Sterculie pruriens* (Lower)	31,890	6.6	
SMF	*Inga macrophylla–Guarea guara* (Seasonal)	501	0.1	
LMF-MF	*Transitional lower montane to montane*	74	0	
MF	*Richeria grandis–Eschweilera trinitensis* (Montane Cloud)	1266	0.3	
	Forested wetland	12,325	2.6	3.6
ESM	Mangrove	7492	1.6	
ESP	Palm swamp – *Roystonea oleracea* or *Mauritia flexuosa*	1516	0.3	
ESS	Swamp forest – *Pterocarpus officinalis*	267	0.1	
ESS-Cca	Swamp forest – Cca ecotone	908	0.2	
EMF	Marsh forest – *Manicaria saccifera–Jessenia oligocarpa – Euterpe langloisii*	912	0.2	
EM-Cco	Marsh forest – Cco ecotone	693	0.1	
ESO	Other woody wetland	537	0.1	
	Young secondary forest	124,283	26.3	36.3
YSF	Young secondary forest	18,592	3.9	
YSF-Wag	Young secondary forest and abandoned or semi-active woody agriculture	78,832	16.3	
YSF-C	Young secondary forest – former coconut plantation	2229	0.5	
YSF-B	*Bambusa vulgaris*	21,013	4.4	
Br	*Hevea brasiliensis* – former plantation	3617	0.8	
	Tree plantations	11,244	2.4	3.3
PT	*Tectona grandis*	8694	1.8	
PP	*Pinus caribaea*	2504	0.5	
PO	Other plantation	46	0	
	Total forest area	342,409	72.6	
	Emergent wetlands and wet savanna	11,075	2.3	
EMS	Wet savanna, with or without shrubs	277	0.1	
ESH	Herbaceous wetland and wet savannah	5022	1	
EAg	Seasonally flooded herbaceous agriculture (active or inactive)	5776	1.2	
	Recently active agriculture, pasture (excluding wetland agriculture	83,933	17.8	
WA	Active woody agriculture	3073	0.6	
WAC	Active woody agriculture – coconut	2709	0.6	
Agric	Grassy areas, herbaceous agriculture or pasture (including former sugar cane)	65,475	13.6	
FC	Recently inactive sugar cane	12,676	2.6	
	Non-vegetated	5639	1.2	
	Quarry	1658	0.3	
	Coastal sand and rock	504	0.1	
	Pitch lake	52	0.6	
	Bare ground and bulldozed land	388	0.1	
	Water – permanent	3037	0.6	
	Urban – high or medium density	8695	1.8	
	Urban – low density	31,029	6.4	
	Urban grass	406	0.1	
	Urban and built-up	40,130	8.5	
	Total area (forest and nonforest)	471,942		

Greater Antilles, and because the presence of serpentintized rocks on Tobago has not been previously mentioned in the literature on Tobago's vegetation, a botanical survey of Tobago's xerophytic rain forests could be warranted.

4.2.3. Influence of multiseason, multidecade imagery on predicting forest association

In lowland Trinidad, the decision-tree model of forest association that uses both the early dry season imagery from 2007, plus

Table 8
Areas of land cover and forest type for Tobago.

Symbol	Tobago forest type and land cover	Area (ha)	Percent of Trinidad	Percent of Forest
	Dry evergreen, deciduous and semi-evergreen forests	5775	19	23
LWS	*Coccoloba uvifera – Hippomane mancinella* (dry evergreen littoral)	136	0.5	
XFBa	*Manilkara bidentata* (dry evergreen Littoral)	194	0.6	
Ssd	*Bursera simaruba–Coccothrinax barbadensis* (deciduous)	1271	4.2	
Sch	*Hura crepitans – Tabebuia chrysantha – Spondias mombin* (semi-evergreen)	4174	13.9	
	Rain forest	10,347	34	41
XFBb	*Manilkara bidentata – Guettarda scabra* (xerophytic)	937	3.1	
LMF	*Licania biglandulosa – Byrsonima spicata* (lower montane)	4566	15.2	
Ccp	*Carapa guianensis – Euterpe precatoria* (lowland)	4844	16.1	
	Young secondary forests	8798	29	35
	Young secondary forest	7038	23	
	Young secondary forest – former *Cocos nucifera* plantation	133	0.4	
	Young secondary forest – *Bambusa vulgaris*	1627	5.4	
	Forested wetlands	228	0.8	0.9
	Mangrove	216	0.7	
	Other woody wetland	12	0	
	Total forest area	25,148		
	Herbaceous wetland	7	0	
	Agriculture, grassy areas and pasture	2156	7.2	
	Active woody agriculture	71	0.2	
	Active woody agriculture – coconut	10	0	
	Grassy areas, herbaceous agriculture or pasture	2075	6.9	
	Nonvegetated	235	0.8	
	Quarry	24	0.1	
	Coastal sand and rock	115	0.4	
	Bare ground and bulldozed land	57	0.2	
	Water – permanent	39	0.1	
	Urban or Built-up	2556	8.5	
	Urban – high or medium density	178	0.6	
	Urban – low density	2206	7.3	
	Urban grass	172	0.6	
	Total area (forest and nonforest)	30,095		

all of the late-dry season mosaics from the 1980s, correctly classifies 93% of all test pixels (Kappa = 0.92 ± 0.01). This result is highly significantly different from the 86% accuracy for models that excluded the 1980s imagery ($p \ll 0.0001$) (Kappa = 0.84 ± 0.01) (Table 5). It is also significantly different from ($p \ll 0.0001$), but only slightly more than, the Kappa coefficient for models that include only the mosaics from 1985 or 1986 ($p < 0.005$), but it is not significantly different from the model that included only the mosaic from the drought (1987). At the class level, excluding all of the late dry season data results in significantly different and lower overall accuracy for all semi-evergreen and most seasonal evergreen associations and for the older secondary forest class (young secondary forest and abandoned woody agriculture, or YSF-Wag).

In the mountainous Northern Range of Trinidad, if at least one mosaic from the 1980s is included in a decision-tree model, overall classification model accuracy is no different than if all of the 1980s mosaics are included. If no mosaics from the 1980s are included, overall classification accuracy for deciduous forest and one young secondary forest class (YSF-Wag) are significantly different ($p < 0.005$) and smaller. These results do not reflect the fact that montane seasonal forest was only visually distinct in the drought-year image, because we manually delineated that class.

Including the 1980s mosaics results in large relative increases in overall accuracy at the class level for some classes, even when the overall accuracy calculated across all classes is only slightly larger (Table 6). In the Trinidad lowlands, relative accuracy of semi-evergreen forest classes is 7–36% larger when one or more of the 1980s mosaics are used in the models. Smaller relative increases of 3 to 11% occur for seasonal evergreen classes. The secondary forest class YSF-Wag is 5–6% more accurate in two combinations of

mosaics that include 1980s data. In the Northern Range, deciduous forest accuracy is 14–21% greater if 1980s data are included; YSF-Wag accuracy is 5–9% larger for three combinations of mosaics that include 1980s data. In general, classifications were most accurate if the models included a mosaic with a reference scene from early May, the absolute end of the dry season (1986, 1987), particularly that from the 1987 drought.

4.3. Areas of land cover and forest types in Trinidad and Tobago

Trinidad is 73% forested, 8% urban and 18% active or inactive herbaceous agriculture or pasture (Fig. 3, Table 7). Sugar-cane fields that are no longer cultivated compose at least 2.6% of Trinidad's land area and most of the wetlands converted to agriculture. Thirty-six % of forests are mature seasonal evergreen forests, 36% are young secondary forests, 10% are mature montane forests, 7% are mature semi-evergreen forests and 4% are forested wetlands. Stands with >60% cover of the nonnative bamboo, *Bambusa vulgaris*, compose 4.4% of Trinidad's area (6% of its forests). The mature forests include much old-growth forest or forest subject only to selective logging or wildfire.

Tobago is 84% forested, 8.5% urban and 7.2% agriculture or grassy areas (Fig. 4, Table 8). The most extensive forest types in Tobago are lowland and lower montane rain forests, young secondary forests and well-developed but secondary semi-evergreen forests. Of Tobago's other forests, 3% are xerophytic rain forests and 4% are deciduous seasonal forests. Nonnative bamboo forests occupy 5% of Tobago and 6% of all forest. The lower montane and xerophytic rain forests are believed to have not been subject to clearing for agriculture before 1944 (Beard, 1944a,b).

5. Discussion and conclusions

5.1. Mapping tropical forest associations with gap-filled Landsat imagery and Google Earth-enabled selection of training data

Our results highlight that tropical tree communities can be mapped to the level of forest association with "noisy" gap-filled Landsat imagery, at least if, as in this study (1) extensive training data can be collected that represent the spectral and spatial variability of each association; (2) sufficient ancillary data are available – the temperature and topographic data that we used are available for all of the tropics; and (3) characteristics of associations, like deciduousness as reflected in multiseason imagery, allow discrimination among a known set of tree communities.

With field data, historical maps for public lands, and detailed descriptions of forest associations, we learned to identify most of the tree communities in the fine resolution imagery viewable with Google Earth. We discovered that a large portion of the forest associations were distinct in the fine resolution imagery viewable there because of unique growth form or canopy structure. Other associations had distinct leaf or flowering phenology that was visible in certain seasons, and the appropriate season of imagery was often also viewable with Google Earth. The multiseason views there allowed us to collect enough training data to compensate for the noise in gap-filled imagery and the complex spatial distributions of forest types.

5.2. Synthetic multiseason, multidecade Landsat imagery, particularly from droughts, are important

We found that multiseason Landsat imagery from the late dry season, even when it was gap-filled synthetic multiseason imagery, significantly improved mapping of tropical forest associations that differ in the numbers of tree species and individuals that are deciduous. Multispectral satellite imagery is specifically designed to detect differences in vegetation greenness and consequently well suited to discriminate floristic associations that differ in deciduousness. In many landscapes, ancillary data on environmental variables will be required to map different forest classes. In some cases, however, spectral data may better reflect these differences than ancillary data can. This is particularly important where topography does not strongly predict forest type, as is the case in Trinidad's lowlands. The multiseason imagery helps delineate the spatial distributions of some associations where available rainfall maps do not have sufficient spatial resolution to help distinguish finer-scale patterns in forest type, as in this study. Other classes were most distinct in wet-season imagery, including the xerophytic rain forests of Tobago, which we found here are closely associated with ultramafic geology.

Our results also highlight the value of class-specific comparisons when evaluating differences in classification accuracy. Overall accuracy is more typically evaluated, but in this study the largest improvements from adding multiseason imagery were at the class level. Although this seems obvious, it is not always considered.

With multidecade imagery, imagery from past climate extremes or from stand-clearing disturbances can help classify forests in current imagery. Here we discovered that Landsat imagery from a past drought is better for distinguishing forest associations that are spectrally similar in the average image for most dates. The boundaries between several associations are most distinct, or are only distinct, in imagery from the late dry season of a severe drought. Droughts, floods, or other climatic events that are not annual events may still shape community composition. Stand-clearing disturbances can also affect tree species composition, and in this study older imagery also improved detection of older secondary forest and abandoned woody agriculture.

5.3. Mapping low-density urban lands

The thermal band did not much improve mapping of low-density urban lands, similar to general understanding (Yang et al., 2003). But model accuracy for low-density urban lands was better than in our prior work (Helmer et al., 2008; Kennaway et al., 2008). The improved accuracy for low-density urban lands probably stems from a more restricted selection of training data to Landsat pixels that clearly reflected a mixture of natural vegetation and built-up lands. We did not attempt to include with this class pixels with as little as 15% cover of man-made structures as in the prior work. The strategy produced visually and statistically excellent results.

5.4. Approach potential and limitations

Though we used specialized software to produce the gap-filled imagery and apply the decision-tree classification models, alternatives will soon be freely available with Google Earth Engine (GEE) (http://earthengine.google.org). It is expected that GEE will allow users to make a composite Landsat image, input classification training points collected from Google Earth, and then apply the points to classify one or more dates of Landsat imagery with a machine learning algorithm. Other Landsat image products may also become available over time. Roy et al. (2010), for example, produced gap-filled Landsat imagery for the US. Similar gap-filled data could soon become globally available.

Persistent cloudiness affects forest mapping in many tropical forest landscapes, and the scan gaps in Landsat 7 imagery have added to the need for combining many scenes to cover an area (Trigg et al., 2006; Lindquist et al., 2008). In Trinidad and Tobago, many floristic differences are associated with physiognomic differences in deciduousness or inundation that are visible in Landsat imagery from certain times. This relationship between floristics and physiognomic features that are detectable in multiseason imagery is likely to be repeated elsewhere. To the extent that synthetic gap-filled Landsat imagery can be created that reflects these differences, the approach here may be applicable elsewhere.

A limitation to this approach is that in remote places, fine resolution images viewable with Google Earth are still limited to one season or only a portion of each Landsat scene. This drawback, however, will be less important as the global archive of fine resolution imagery increases and in more uniform landscapes, samples of fine resolution imagery may be sufficient. Floristic classifications based on data as comprehensive as that for Trinidad and Tobago are not available for all tropical forests. However, 20th century ecologists have described many of the major tropical tree communities, and these descriptions may be useful where there has not been large-scale disturbance since those studies. Another consideration is that floristic differences between adjacent classes may not always be clearly identifiable from differences in phenology or disturbance history. For example, gradual changes in species composition may be difficult to define when collecting classification training data from fine resolution imagery.

Appendix A. Supplementary material

Supplementary data associated with this article can be found, in the online version, at http://dx.doi.org/10.1016/j.foreco.2012.05.016.

References

Aide, T.M., Zimmerman, J.K., Rosario, M., Marcano, H., 1996. Forest recovery in abandoned cattle pastures along an elevational gradient in northeastern Puerto Rico. Forest Ecology and Management 28, 537–548.

Beard, J.S., 1944a. The natural vegetation of Tobago, British West Indies. Ecological Monographs 14, 135–163.

Beard, J.S., 1944b. Climax vegetation in Tropical America. Ecology 25, 127–158.

Beard, J.S., 1946a. The Natural Vegetation of Trinidad. Oxford Univeristy Press, Oxford.

Beard, J.S., 1946b. The mora forests of Trinidad, British West Indies. Journal of Ecology 33, 173–192.

Bohlman, S.A., Adams, J.B., Smith, M.O., Peterson, D.L., 1998. Seasonal foliage changes in the eastern Amazon basin detected from Landsat Thematic Mapper satellite images. Biotropica 30, 13–19.

Brown, M., Lewis, H.G., Gunn, S.R., 2000. Linear spectral mixture models and support vector machines for remote sensing. IEEE Transactions on Geoscience and Remote Sensing 38, 2346–2360.

Cedeño-Maldonado, J.A., Breckon, G.J., 1996. Serpentine endemism in the flora of Puerto Rico. Caribbean Journal of Science 32, 348–356.

Chen, K.S., Tzeng, Y.C., Chen, C.F., Kau, W.L., 1995. Land-cover classification of multispectral imagery using a dynamic learning neural network. Photogrammetric Engineering & Remote Sensing 61, 403–408.

Chen, J., Zhu, X., Vogelmann, J.E., Gao, F., Jin, S., 2011. A simple and effective method for filling gaps in Landsat ETM+ SLC-off images. Remote Sensing of Environment 115, 1053–1064.

Chinea, J.D., 2002. Tropical forest succession on abandoned farms in the Humacao Municipality of eastern Puerto Rico. Forest Ecology and Management 167, 195–207.

Chinea, J.D., Helmer, E.H., 2003. Diversity and composition of tropical secondary forests recovering from large-scale clearing: results from the 1990 inventory in Puerto Rico. Forest Ecology and Management 180, 227–240.

Choi, H., Bindschadler, R., 2004. Cloud detection in Landsat imagery of ice sheets using shadow matching technique and automatic normalized difference snow index threshold value decision. Remote Sensing of Environment 91, 237–242.

Chust, G., Chave, J., Condit, R., Aguilar, S., Lao, S., Pérez, R., 2006. Determinants and spatial modeling of tree β-diversity in a tropical forest landscape in Panama. Journal of Vegetation Science 17, 83–92.

Crist, E.P., Cicone, R.C., 1984. A physically-based transformation of Thematic Mapper data – the TM Tasseled Cap. IEEE Transactions on Geoscience and Remote Sensing 22, 256–263.

Day, M.J., Chenoweth, M.S., 2004. The Karstlands of Trinidad and Tobago, their land use and conservation. The Geographical Journal 170, 256–266.

Donovan, S.K., 1994. Trinidad. In: Donovan, S.K., Jackson, T.A. (Eds.), Caribbean Geology, An Introduction. The University of the West Indies Publishers' Association, Kingston, Jamaica, pp. 209–228.

Estrada, M., 2011. Standards and methods available for estimating project-level REDD+ carbon benefits: reference guide for project developers, Working Paper 52. Center for International Forestry Research, Bogor, Indonesia.

Ewel, J.J., Whitmore, J.L., 1973. The Ecological Life Zones of Puerto Rico and the U.S. Virgin Islands. Institute of Tropical Forestry, Rio Piedras, Puerto Rico, p. 72.

Farr, T.G., Rosen, P.A., Caro, E., Crippen, R., Duren, R., Hensley, S., Kobrick, M., Paller, M., Rodriguez, E., Roth, L., Seal, D., Shaffer, S., Shimada, J., Umland, J., Werner, M., Oskin, M., Burbank, D., Alsdorf, D., 2007. The shuttle radar topography mission. Reviews of Geophysics 45, RG2004.

Foody, G.M., 2009. Classification accuracy comparison: hypothesis tests and the use of confidence intervals in evaluations of difference, equivalence and non-inferiority. Remote Sensing of Environment 113, 1658–1663.

Foody, G.M., McColloch, M.B., Yates, W.B., 1995. Classification of remotely sensed data by an artificial neural network: issues related to training data characteristics. Photogrammetric Engineering & Remote Sensing 61, 391–401.

FRIM, 1992. Forest Resource Inventory and Management Section Inventory of the Indigenous Forest of Trinidad. Lands and Surveys Division, Ministry of Planning and Development, Forestry Division.

Gond, V., Freycon, V., Molino, J.-F., Brunaux, O., Ingrassia, F., Joubert, P., Pekel, J.-F., Prévost, M.-F., Thierron, V., Trombe, P.-J., Sabatier, D., 2011. Broad-scale spatial pattern of forest landscape types in the Guiana Shield. International Journal of Applied Earth Observation and Geoinformation 13, 357–367.

Google, 2010. Google Earth. Google, Inc., Mountain View, CA.

Hansen, M., Dubayah, R., Defries, R., 1996. Classification trees: an alternative to traditional land cover classifiers. International Journal of Remote Sensing 17, 1075–1081.

Hansen, M.C., Roy, D.P., Lindquist, E., Adusei, B., Justice, C.O., Altstatt, A., 2008. A method for integrating MODIS and Landsat data for systematic monitoring of forest cover and change in the Congo Basin. Remote Sensing of Environment 112, 2495–2513.

Hardisky, M.A., Klemas, V., Smart, R.M., 1983. The influence of soil salinity, growth form, and leaf moisture on the spectral reflectance of Spartina alterniflora canopies. Photogrammetric Engineering & Remote Sensing 49.

Helmer, E.H., Ruefenacht, B., 2005. Cloud-free satellite image mosaics with regression trees and histogram matching. Photogrammetric Engineering & Remote Sensing 71, 1079–1089.

Helmer, E.H., Ruefenacht, B., 2007. A comparison of radiometric normalization methods when filling cloud gaps in Landsat imagery. Canadian Journal of Remote Sensing/Journal Canadien de Teledetection 33, 325–340.

Helmer, E.H., Cohen, W.B., Brown, S., 2000. Mapping montane tropical forest successional stage and land use with multi-date Landsat imagery. International Journal of Remote Sensing 21, 2163–2183.

Helmer, E.H., Ramos, O., Lopez, T.D.M., Quiñones, M., Diaz, W., 2002. Mapping forest type and land cover of Puerto Rico, a component of the Caribbean biodiversity hotspot. Caribbean Journal of Science 38, 165–183.

Helmer, E.H., Kennaway, T.A., Pedreros, D.H., Clark, M.L., Marcano-Vega, H., Tieszen, L.L., Ruzycki, T.R., Schill, S., Carrington, C.M.S., 2008. Land cover and forest formation distributions for St. Kitts, Nevis, St. Eustatius, Grenada and Barbados from decision tree classification of cloud-cleared satellite imagery. Caribbean Journal of Science 44, 175–198.

Helmer, E.H., Lefsky, M.A., Roberts, D.A., 2009. Biomass accumulation rates of Amazonian secondary forest and biomass of old-growth forests from Landsat time series and the Geoscience Laser Altimeter System. Journal of Applied Remote Sensing 3, 033505:033501–033531.

Helmer, E.H., Ruzycki, T.S., Wunderle Jr, J.M., Voggesser, S., Ruefenacht, B., Kwit, C., Brandeis, T.J., Ewert, D.N., 2010. Mapping tropical dry forest height, foliage height profiles and disturbance type and age with a time series of cloud-cleared Landsat and ALI image mosaics to characterize avian habitat. Remote Sensing of Environment 114, 2457–2473.

Hijmans, R.J., Cameron, S.E., Parra, J.L., Jones, P.G., Jarvis, A., 2005. Very high resolution interpolated climate surfaces for global land areas. International Journal of Climatology 25, 1965–1978.

Holdridge, L.R., 1967. Life Zone Ecology. Tropical Science Center, San José, Costa Rica.

Howard, S.M., Lacasse, J.M., 2004. An evaluation of gap-filled Landsat SLC-off imagery for wildland fire burn severity mapping. Photogrammetric Engineering & Remote Sensing 70, 877–880.

Huang, C., Wylie, B., Homer, C., Yang, L., Zylstra, G., 2002. Derivation of a Tasseled Cap transformation based on Landsat 7 at-satellite reflectance. International Journal of Remote Sensing 23, 1741–1748.

Jackson, T.A., Donovan, S.K., 1994. Tobago. In: Donovan, S.K., Jackson, T.A. (Eds.), Caribbean Geology, An Introduction. The University of the West Indies Publishers' Association, Kingston, Jamaica, pp. 193–207.

Jennings, M.D., Faber-Langendoen, D., Loucks, O.L., Peet, R.K., Roberts, D., 2009. Standards for associations and alliances of the U.S. National Vegetation Classification. Ecological Monographs 79, 173–199.

Kennaway, T., Helmer, E.H., 2007. The forest types and ages cleared for land development in Puerto Rico. Geoscience and Remote Sensing 44, 356–382.

Kennaway, T.A., Helmer, E.H., Lefsky, M.A., Brandeis, T.A., Sherrill, K.R., 2008. Mapping land cover and estimating forest structure using satellite imagery and coarse resolution lidar in the Virgin Islands. Journal of Applied Remote Sensing 2 (023551), pp. 023551–023551.

Kimes, D.S., Nelson, R.F., Salas, W.A., Skole, D.L., 1999. Mapping secondary tropical forest and forest age from SPOT HRV data. International Journal of Remote Sensing 20, 3625–3640.

Larkin, C.C., Kwit, C., Wunderle, J.M., Helmer, E.H., Stevens, M.H.H., Roberts, M.T.K., Ewert, D.N., 2012. Disturbance type and plant successional communities in Bahamian dry forests. Biotropica 44, 10–18.

Lees, B., Ritman, K., 1991. Decision-tree and rule-induction approach to integration of remotely sensed and GIS data in mapping vegetation in disturbed or hilly environments. Environmental Management 15, 823–831.

Lindquist, E.J., Hansen, M.C., Roy, D.P., Justice, C.O., 2008. The suitability of decadal image data sets for mapping tropical forest cover change in the Democratic Republic of Congo: implications for the global land survey. International Journal of Remote Sensing 29, 7269–7275.

Manis, G., Lowry, J., Ramsey, R.D., 2002. Pre-classification: An Ecologically Predictive Landform Model. College of Natural Resources, Utah State University, Logan, UT, p. AML script.

Maxwell, J.C., 1948. Geology of Tobago, British West Indies. Geological Society of America Bulletin 59, 801–854.

Nelson, H.P., 2004. Tropical Forest Ecosystems of Trinidad: Ecological Patterns and Public Perceptions. Wildlife Ecology and Forestry. University of Wisconsin, Madison, Wisconsin, p. 459.

Nelson, R., Boudreau, J., Gregoire, T.G., Margolis, H., Næsset, E., Gobakken, T., Ståhl, G., 2009. Estimating Quebec provincial forest resources using ICESat/GLAS. Canadian Journal of Forest Research 39, 862–881.

NGA, 2003. SRTM Water Body Dataset (SWBD). National Geospatial Intelligence Agency (distributed by the US Geological Survey Center for EROS).

Oatham, M.P., Boodram, N., 2006. The dry forest vegetation communities of Little Tobago Island, West Indies: floristic affinities. Tropical Ecology 47, 211–228.

Ohmann, J.L., Gregory, M.J., 2002. Predictive mapping of forest composition and structure with direct gradient analysis and nearest-neighbor imputation in coastal Oregon, U.S.A. Canadian Journal of Forest Research 32, 725–741.

Phelps, J., Webb, E.L., Agrawal, A., 2010. Does REDD+ threaten to recentralize forest governance? Science 328, 312–313.

Pyke, C.R., Condit, R., Aguilar, S., Lao, S., 2001. Floristic composition across a climatic gradient in a neotropical lowland forest. Journal of Vegetation Science 12, 553–566.

Roy, D.P., Ju, J., Lewis, P., Schaaf, C., Gao, F., Hansen, M., Lindquist, E., 2008. Multi-temporal MODIS-Landsat data fusion for relative radiometric normalization, gap filling, and prediction of Landsat data. Remote Sensing of Environment 112, 3112–3130.

Roy, D.P., Ju, J., Kline, K., Scaramuzza, P.L., Kovalskyy, V., Hansen, M., Loveland, T.R., Vermote, E., Zhang, C., 2010. Web-enabled Landsat Data (WELD): Landsat ETM+ composited mosaics of the conterminous United States. Remote Sensing of Environment 114, 35–49.

Ruefenacht, B., Finco, M.V., Nelson, M.D., Czaplewski, R., Helmer, E.H., Blackard, J.A., Holden, G.R., Lister, A.J., Salajanu, D., Weyermann, D., Winterberger, K., 2008. Conterminous US and Alaska forest type mapping using forest inventory and analysis data. Photogrammetric Engineering & Remote Sensing 74, 1379–1388.

Sader, S.A., Legaard, K.R., 2008. Inclusion of forest harvest legacies, forest type, and regeneration spatial patterns in updated forest maps: a comparison of mapping results. Forest Ecology and Management 255, 3846–3856.

Scott, J.M., Davis, F., Csuti, G., Noss, R., Butterfield, B., Groves, C., Anderson, H., Caicco, S., D'Erchia, F., Edwards, T.C., Ulliman, J., Wright, R.G., 1993. Gap analysis: a geographical approach to protection of biological diversity. Wildlife Monographs 123, 1–41.

Scott, P.W., Jackson, T.A., Dunham, A.C., 1999. Economic potential of the ultramafic rocks of Jamaica and Tobago: two contrasting geological settings in the Caribbean. Mineralium Deposita 34, 718–723.

Sesnie, S.E., Gessler, P.E., Finegan, B., Thessler, S., 2008. Integrating Landsat TM and SRTM-DEM derived variables with decision trees for habitat classification and change detection in complex neotropical environments. Remote Sensing of Environment 112, 2145–2159.

Skidmore, A.K., 1989. An expert system classifies eucalypt forest types using thematic mapper data and a digital terrain model. Photogrammetric Engineering & Remote Sensing 55, 1449–1464.

Snoke, A.W., Rowe, D.W., Yule, J.D., Wadge, G., 2001a. Petrologic and structural history of Tobago, West Indies: a fragment of the accreted Mesozoic oceanic arc of the southern Caribbean. Geological Society of America Special Papers 354, 1–54.

Snoke, A.W., Rowe, D.W., Yule, J.D., Wadge, G., 2001b. Geologic Map of Tobago, West Indies with Explanatory Notes. Geological Society of America Map and Chart Series 087, p. 1 Sheet and 24 p Pamphlet.

Suter, H.H., 1960. The General and Economic Geology of Trinidad. B.W.I. HMSO, London.

Tottrup, C., 2004. Improving tropical forest mapping using multi-date Landsat TM data and pre-classification image smoothing. International Journal of Remote Sensing 25, 717–730.

Trigg, S.N., Curran, L.M., McDonald, A.K., 2006. Utility of Landsat 7 satellite data for continued monitoring of forest cover change in protected areas in Southeast Asia. Singapore Journal of Tropical Geography 27, 49–66.

Wertz-Kanounnikoff, S., Kongphan-apirak, M., 2009. Emerging REDD+: a Preliminary Survey of Demonstration Readiness Activities, Working Paper 46. Center for International Forestry Research, Bogor, Indonesia.

Wulder, M.A., Ortlepp, S.M., White, J.C., Maxwell, S., 2008. Evaluation of Landsat-7 SLC-off image products for forest change detection. Canadian Journal of Remote Sensing 34, 93–99.

Yang, L., Huang, C., Homer, C.G., Wylie, B.K., Coan, M.J., 2003. An approach for mapping large-area impervious surfaces: synergistic use of Landsat-7 ETM+ and high spatial resolution imagery. Canadian Journal of Remote Sensing 29, 230–240.